Assessing suitability of sites near Pine Island Glacier for subglacial bedrock drilling aimed at detecting Holocene retreat-readvance

Joanne S. Johnson[1], John Woodward[2], Ian Nesbitt[3], Kate Winter[2], Seth Campbell[3], Keir A. Nichols[4], Ryan A. Venturelli[5], Scott Braddock[3], Brent M. Goehring[6], Brenda Hall[3], Dylan H. Rood[4], Greg Balco[7,8]

[1]British Antarctic Survey, Cambridge, CB3 0ET, UK
[2]Department of Geography and Environmental Sciences, Northumbria University, Newcastle-upon-Tyne, NE1 8ST, UK
[3]School of Earth and Climate Sciences and the Climate Change Institute, University of Maine, Orono, ME 04469, USA
[4]Department of Earth Science and Engineering, Imperial College London, London SW7 2AZ, UK
[5]Department of Geology and Geological Engineering, Colorado School of Mines, Golden, CO 80401, USA
[6]Los Alamos National Laboratory, Los Alamos, NM 87545, USA
[7]Lawrence Livermore National Laboratory, P.O. Box 808, Livermore, CA 94551, USA
[8]Berkeley Geochronology Center, Berkeley, CA 94709, USA

Correspondence to: Joanne S. Johnson (jsj@bas.ac.uk)

Abstract. Unambiguous identification of past episodes of ice sheet thinning below the modern surface and grounding-line retreat inboard of present requires recovery and exposure dating of subglacial bedrock. Such efforts are needed to understand the significance and potential future reversibility of ongoing and projected change in Antarctica. Here we evaluate the suitability for subglacial bedrock drilling of sites in the Hudson Mountains, in the Amundsen Sea sector of West Antarctica. We use an ice sheet model and field data − geological observations, glaciological observations and bedrock samples from nunataks, and ground-penetrating radar from subglacial ridges − to rate each site against four key criteria: i) presence of ridges extending below the ice sheet, ii) likelihood of increased exposure of those ridges if the grounding line was inboard of present, iii) suitability of bedrock for drilling and geochemical analysis, and iv) accessibility for aircraft and drilling operations. Our results demonstrate that although no site in the Hudson Mountains is perfect for this study when assessed against all criteria, the accessibility, N-S orientation and basaltic bedrock lithology of Winkie Nunatak's southernmost ridge (74.86°S / 99.77°W) make it a feasible site both for drilling and subsequent cosmogenic nuclide analysis. Furthermore, the ridge is strewn with glacial erratics at all elevations, providing valuable constraints on its early Holocene deglacial history. Based on our experiences during this study, we conclude with a series of recommendations for assessing site suitability for future bedrock drilling campaigns. We emphasise the importance of consulting a range of expertise prior to drilling and ensuring that sufficient field reconnaissance is undertaken (including obtaining detailed grids of radar survey data and bedrock samples).

1 Introduction

This paper describes geological and glaciological considerations needed for choosing a suitable site for a subglacial bedrock drilling campaign aimed at determining if (and when) the Antarctic ice sheet was ever smaller in the recent geological past

than it is today. Such considerations are broadly applicable to any similar study (Johnson et al., 2022), but we focus here on part of the Pine Island-Thwaites Glacier system in the Amundsen Sea sector of Antarctica, due to its known instability (Joughin et al. 2014). Ice mass loss from Pine Island, Thwaites and surrounding glaciers is accelerating, and between 2003 and 2019 these glaciers contributed 7.5 mm to global sea level rise, dominating the total contribution from Antarctica during that period (Smith et al., 2020). However, there is only limited direct evidence for changes in ice sheet thickness in the Pine Island-Thwaites Glacier system between the mid-Holocene (~5,000 years ago) and the onset of 20th-century satellite observations (Balco et al., 2023). Hence, it is currently unknown whether (i) ice sheet changes similarly rapid to those of the past decades occurred more widely in the Amundsen Sea sector during the late Holocene, and (ii) such rapid changes should be regarded as exceptional with respect to pre-observational history. These uncertainties limit our understanding of the drivers for such events (Jones et al., 2022). Determining whether the grounding line in this region ever retreated inboard of its present position during the past few millennia and subsequently readvanced (hereafter termed "retreat-readvance") is necessary for understanding the possible range of glacier behaviours and mechanisms for recovery that could occur under the climatic conditions predicted for the next few centuries (Meredith et al., 2019). Similar studies are urgently needed elsewhere in Antarctica to determine how widespread Holocene retreat-readvance of the ice sheet was, its extent and timing, and what drove such changes.

Subglacial drilling enables recovery of bedrock cores (Spector et al., 2018; Braddock et al., 2024) from which the exposure history of the subglacial bedrock surface can be inferred by measuring the concentration of cosmogenic nuclides in minerals (typically quartz) extracted from a variety of depths within the cores (Schaefer et al., 2016). Any detectable presence of in-situ-produced cosmogenic nuclides in subglacial bedrock, with an exponential decrease in concentration with depth, would imply that the bedrock experienced near-surface exposure to cosmic radiation and therefore ice-free conditions, or only very thin ice cover (see Balco et al., 2023), in the past (Spector et al., 2018). The extent of ice sheet thinning below present at that time can be determined by collecting a series of bedrock cores along a transect trending inland perpendicular to the grounding line. This approach provides the ice sheet thinning history, but the relationship between thinning and associated grounding-line retreat is likely to vary between glaciers due to differences in bathymetric and other boundary conditions (see section 5.3 of Johnson et al., 2021 for discussion). Thus, ice sheet modelling is usually required to establish this relationship for individual sites. Subglacial bedrock recovery efforts have increased in the last decade, with successful attempts in both Antarctica and Greenland aiming to search for evidence of ice sheet collapse during warm periods. These have focused largely on the last interglacial (for example, drilling campaigns in the Pirrit Hills, interior West Antarctica [Kuhl et al., 2020] and Ohio Range, Transantarctic Mountains [Mukhopadhyay et al., 2020]), but three studies to date have sought evidence specifically for Holocene exposure, focusing on the following locations: central Amundsen Sea sector, Antarctica (Balco et al., 2023); southern Weddell Sea sector, Antarctica (Small et al., 2024); West Greenland (Balter-Kennedy et al., 2023). Subglacial sediments documenting grounding-line retreat inboard of present during the Holocene have been recovered by drilling in the Ross Sea sector (Kingslake et al. 2018; Venturelli et al., 2020, 2023).

In the present paper, we describe the results of reconnaissance surveys undertaken prior to a subglacial bedrock drilling campaign in the eastern Amundsen Sea sector of Antarctica, targeting the Hudson Mountains in the Pine Island-Thwaites Glacier system (Fig. 1). These mountains are situated both adjacent to Pine Island Glacier (PIG) and near islands in Pine Island

70   Bay from which Relative Sea Level (RSL) records imply steady retreat of PIG through the late Holocene (Braddock et al., 2022). This steady retreat, however, contrasts with the mid to late Holocene retreat-readvance of Pope Glacier detected using subglacial bedrock at Mt Murphy in the western Pine Island-Thwaites Glacier system (Fig. 1a) (Balco et al., 2023). The Hudson Mountains are thus a good site for testing whether the response of PIG to Holocene climate was similar to that of other glaciers in the region. We describe the approach and criteria we used for choosing a suitable drill site and conclude with some

75   recommendations for assessing sites for similar future studies.
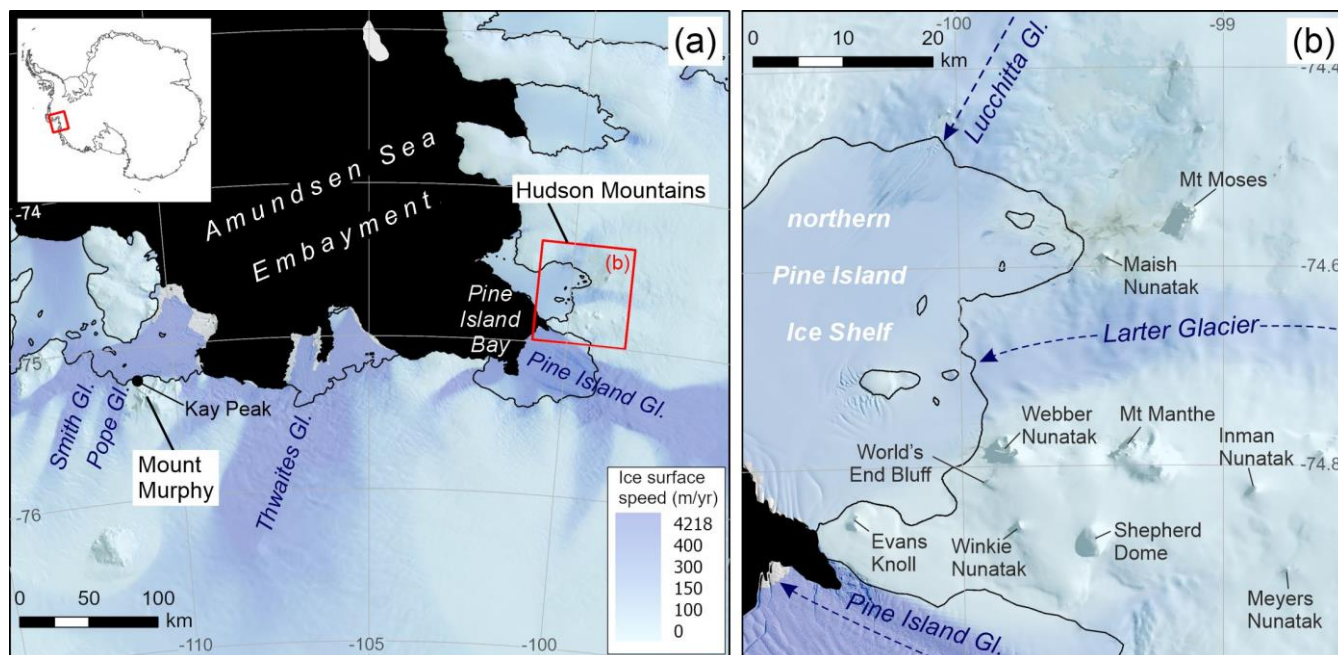
Figure 1: The location of the Hudson Mountains study site within the Amundsen Sea sector of Antarctica. **(a)** Map of Amundsen Sea Embayment, showing location of subglacial bedrock drilling sites near Kay Peak, Mt Murphy (Fig. 2) and Hudson Mountains. **(b)** Location
80   of Hudson Mountains nunataks in relation to major glaciers. The grounding line (black) is from Rignot et al. (2016) and the coastline is from the SCAR Antarctic Digital Database [Accessed 15 May 2024]. Ice surface speeds (Rignot et al., 2017) are overlain on Landsat Image Mosaic of Antarctica (LIMA; Bindschadler et al., 2008) in panel (a) and a Landsat 8 Image acquired on 13 March 2022 (courtesy of USGS) in panel (b).

2 What makes a good subglacial bedrock drill site for detecting Holocene retreat-readvance?

85   A range of geological, glaciological, technical and practical considerations are needed when assessing the suitability of a site for subglacial bedrock recovery drilling (Spector et al., 2018; Briner et al., 2022). Successful detection of past ice sheet thinning from subglacial bedrock requires drilling at a site where (i) grounding-line retreat or mass-balance changes would result in

exposure of bedrock that is currently ice-covered, (ii) evidence for exposure would be preserved during subsequent ice cover, (iii) the bedrock lithology is suitable for both drilling and cosmogenic nuclide measurements, and (iv) safe access for a drill rig and operators is possible. Although other geometries can meet these criteria, commonly, they lead to selection of drill sites on the subglacial extension of exposed mountain ridges (Fig. 2), primarily based on the observation from the modern landscape that ridge tops are more likely to be ice-free than ridge flanks, as well as the relatively high confidence that the rock encountered by drilling will be the same lithology as the exposed ridge.
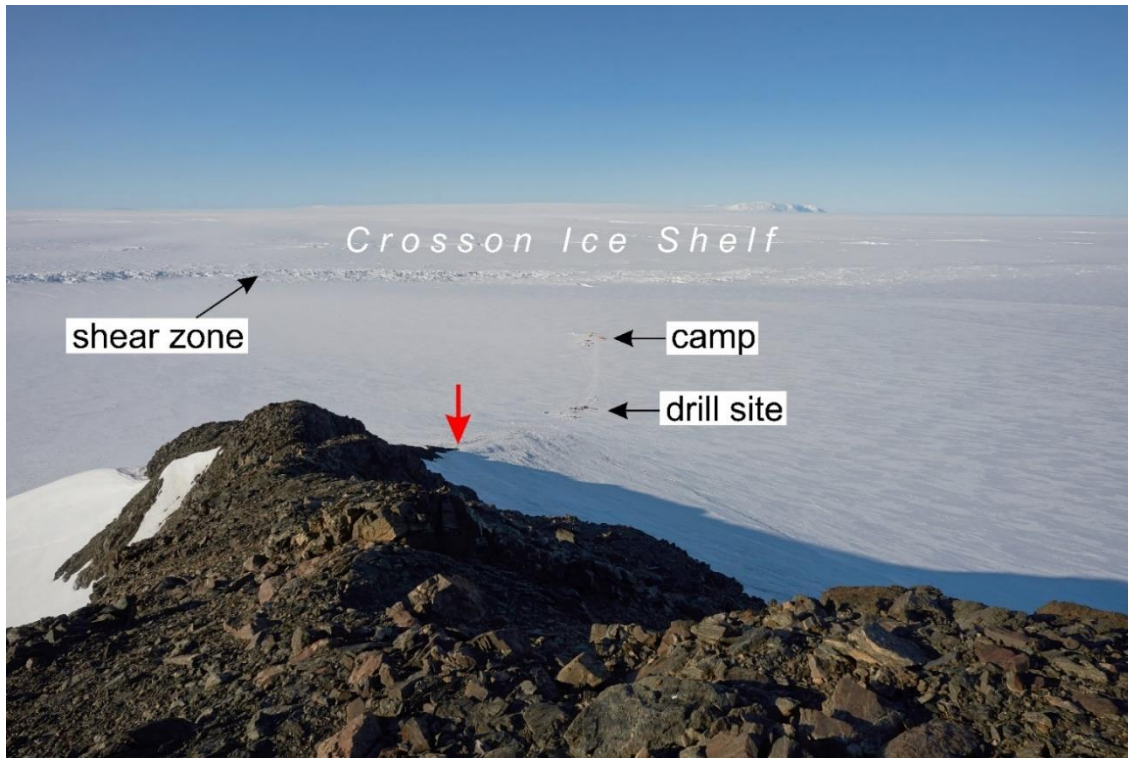
Figure 2: Photograph of a drill site at the Mt Murphy massif in the central Amundsen Sea Embayment. At the location marked by the red downward pointing arrow, the bedrock ridge (foreground) extends north from Kay Peak (Fig. 1a) below the ice sheet surface in a direction perpendicular to the present grounding line less than 2 km away (demarcated by shear zone crevasses). Its orientation and close proximity to the grounding line means that the ridge is likely to have been more exposed during any past episodes of grounding-line retreat than it is at present. Subglacial bedrock cores were recovered from this ridge in 2019-20 (see Balco et al., 2023).

Lithology is important mainly because some common lithologies do not provide suitable targets for cosmogenic nuclide measurement. Of the range of cosmogenic nuclides that can be commonly measured in rock (in situ ^{14}C, ^{10}Be, ^{26}Al, ^{36}Cl, ^{3}He), one – in situ ^{14}C – is particularly well-suited to investigating exposure on Holocene timescales due to its short half-life (Nichols, 2022). Holocene exposure has also been successfully detected using ^{10}Be and ^{26}Al in quartz, ^{36}Cl in feldspar and ^{3}He in olivine and pyroxene. However, all of those nuclides have half-lives that are much longer than the Holocene (^{10}Be, ^{26}Al, ^{36}Cl) or are

stable (^{3}He). Thus, their detection in subglacial bedrock would imply exposure at some point in the past, but in general could not distinguish between evidence of Holocene exposure and exposure that occurred during a prior interglacial that had not been removed by subsequent subglacial erosion. At present, the in situ ^{14}C production rate and extraction procedures are best-known for quartz (e.g. Lifton et al., 2001). In situ ^{14}C measurement has therefore been largely restricted thus far to quartz-bearing rocks. However, it is theoretically possible to measure in situ ^{14}C in olivine (Pigati et al, 2010), and perhaps other mineral phases (Koester & Lifton, 2023), permitting detection of Holocene readvance at sites with non-quartz-bearing bedrock lithologies such as basalt, gabbro and dolerite. Cosmogenic ^{3}He is also routinely measured in olivine and pyroxene, and ^{10}Be measurements have occasionally been performed in both minerals (e.g. olivine: Carracedo et al., 2019, and pyroxene: Balter-Kennedy et al., 2023b; Bergelin et al., 2024). Although neither of these nuclides could unambiguously detect Holocene exposure, they can be used to provide complementary information about the longer-term exposure history of a surface (e.g. Balco et al., 2023). Finally, in samples for cosmogenic nuclide analysis, target minerals must not only be present but must also be of sufficient abundance and grain size (typically > 100 microns) to permit separation and nuclide extraction. Considering the expected low in situ ^{14}C concentrations in subglacial bedrock (see Balco et al., 2023), at least 5 g of quartz or olivine should be targeted for each in situ ^{14}C measurement (Lamp et al., 2019; Pigati et al., 2010).

Given a site with suitable geometry and bedrock lithology, several technical factors are then important. These are mainly related to the fact that pressurised fluid circulation in the borehole is required for rock coring. To achieve fluid circulation, the rock to be cored, the rock-ice interface and the lowermost ~1-2 m of ice overlying the bedrock must be impermeable so that fluid leakage from the borehole cannot occur (Boeckmann et al., 2021). This, in turn, requires that (i) the ice-rock interface is below the freezing point, (ii) the borehole penetrates at least some thickness of ice rather than only permeable firn, and (iii) any permeability, fractures, or joints in basal sediment or bedrock are sealed by ice. Essentially all candidate shallow drilling sites in Antarctica are expected to be frozen at the bed. To date, successful drilling programmes have been carried out both in areas where firn is absent and blue ice is exposed at the surface as well as in areas of firn where the borehole extended below the firn-ice transition depth and bottomed in ice. In addition, bedrock boreholes have been found to be sealed by ice in nearly all subglacial bedrock drilling attempts; the exception was one site in the Ohio Range (Mukhopadhyay et al., 2020) where some fluid was lost into jointed bedrock that was apparently not sealed. Overall, fluid circulation is highly likely to be feasible at any site below the firn-ice transition depth, so from the perspective of site selection, this criterion primarily requires an estimate of the firn thickness (crevasses extending to the bed could also preclude fluid circulation, but such a site would most likely not be safely accessible for drilling, as noted below). Firn thickness is determined by local temperature and accumulation rate and was found to be in the range 15-20 m at Mt Murphy (Balco et al., 2023). As the climate in the Hudson Mountains is similar, sites with firn at the surface there are expected to likewise support rock coring at depths below 15-20 m; sites with exposed blue ice at the surface would allow coring at shallower depths.
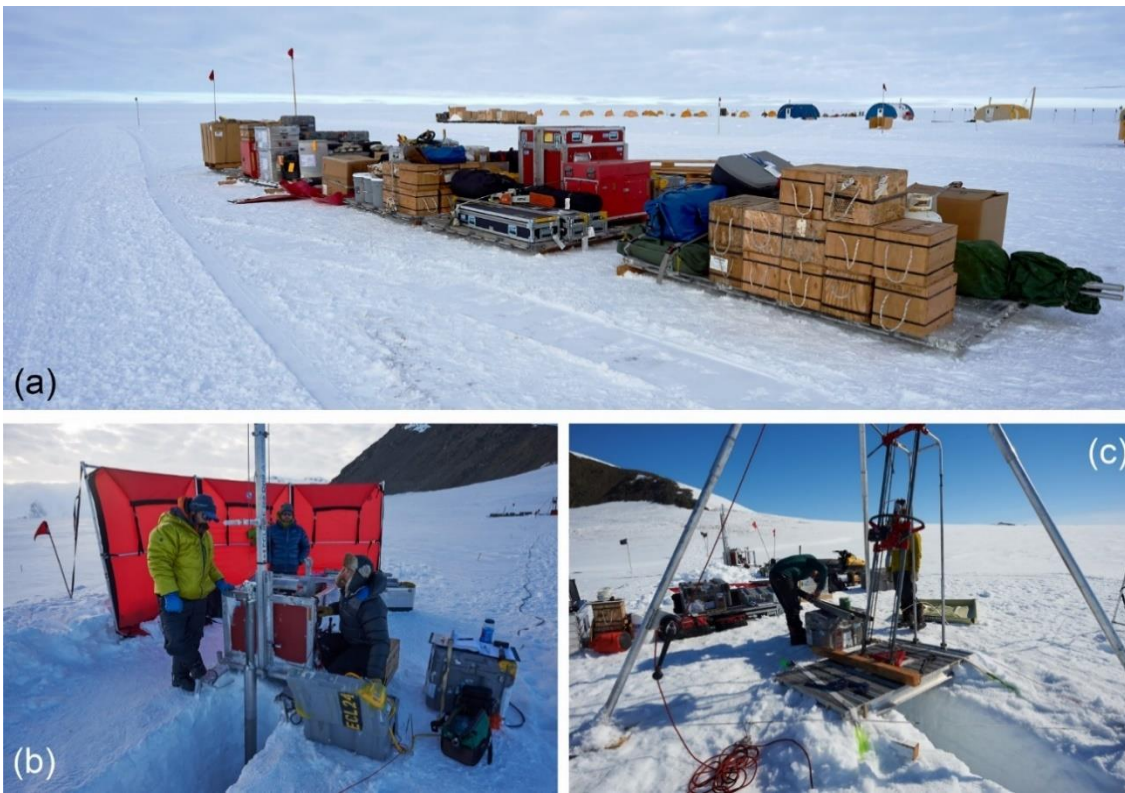
Figure 3: Equipment needed for shallow subglacial bedrock drilling. (a) In the foreground, all cargo (except snowmobiles and fuel) deployed for 2019-20 drilling campaign at Mt Murphy. **(b)** US Ice Drilling Program "Eclipse" ice drill in use at Mt Murphy. **(c)** US Ice Drilling Program "Winkie" drill, and associated equipment. The Eclipse drill is used to drill through ice to access the bedrock whilst the Winkie drill is used for bedrock recovery. Where the bedrock lies beneath clean blue ice, the Winkie drill can be used both to drill through the ice *and* recover the bedrock (see Braddock et al., 2024).

Lastly, a potential drill site must be accessible. Crevassing in and around a drill site can make safe access challenging for both the drill operators and researchers conducting the ground-penetrating radar (GPR) surveys during site selection. Bergschrunds are often present adjacent to ice-free ridges and, even if not presenting a fall hazard, may also preclude drilling at shallow depths. These hazards are most significant in snow- or firn-surfaced areas; in blue ice areas, where snow is scoured away from the ice surface, crevassing can be clearly seen and avoided. Even in the absence of crevassing, the snow or ice surface must be flat enough to allow installation of the drill platform as well as to permit working and staging of equipment near it. In addition, a large flat area within a few kilometres of the drill site is needed to allow ski-equipped aircraft access via a skiway (unless helicopters are used); such access is required to deliver to the site, depending on which drill is to be used, several thousands of kilogrammes of drilling equipment – drill rig, drill rods, power supplies, drilling fluid – as well as standard field camp utilities (see Braddock et al., 2024). Figure 3 shows an example of the cargo needed for shallow subglacial drilling (up to ~100 m depth, as for this study). For deeper drilling, much more equipment (and fuel) is needed, requiring both a longer skiway for use by larger aircraft and a wider expanse of crevasse-free ground around the drill site for safe storage and drill operations.

3 Evaluation of candidate drill sites in the Hudson Mountains

To evaluate the suitability of sites, we undertook the following steps which are described below in the sections indicated: (i) initial evaluation prior to field survey – using existing geological samples/exposure ages, remote-sensed imagery and ice sheet modelling (**3.1**), (ii) ground-based field survey – including geophysical survey, glaciological and geological observations, and bedrock sample collection (**3.2**), (iii) final selection of drill site – using data gathered in (i) and (ii) (**3.3**).

3.1 Evaluation prior to field survey

The Hudson Mountains comprise 17 nunataks (Fig. 1b) dominated by basaltic volcanic rocks, the eruptive age of which is known for only two (Mt Manthe: 8.5 ± 1.0 to 5.6 ± 1.9 Ma, and Velie Nunatak: 3.7 ± 0.2 Ma; whole rock K-Ar dates reported in Rowley et al., 1990). Several have exposed rocky ridges extending below the modern ice surface making them potential drill sites. Prior to fieldwork, we examined both existing geological and geomorphological data from the nunataks and modelling studies to determine an order of priority for field survey.

3.1.1 Holocene exposure history

A temporally and spatially detailed picture of the above-ice exposure history is advantageous when choosing a drill site because this allows us to infer where late Holocene records of ice sheet configuration are most likely to be found (Johnson et al., 2022). Exposure history is determined by measuring the abundance of cosmogenic nuclides in the surfaces of either glacial deposits (cobbles and boulders) perched on the exposed portions of ridges (e.g. Stone et al., 2003; Mackintosh et al., 2007) or bedrock of those ridges (e.g. Johnson et al., 2019; Spector et al., 2019). Our knowledge of the Holocene exposure history of the Hudson Mountains is limited thus far to three studies, only two of which are sufficiently detailed to provide a profile of ice surface lowering (Johnson et al., 2014 and Nichols et al., 2023, cf. Johnson et al., 2008 which reports only two ages from a single feature). Johnson et al. (2014) reports a larger suite of cosmogenic nuclide surface exposure ages from Mt Moses and Maish Nunatak, both situated on the northern side of Larter Glacier (Fig. 1b). Although limited in number and situated within only 10 km of each other, these two nunataks together yielded a very well-constrained exposure history, including an estimate of when the modern ice sheet surface elevation was reached. The results show that, at both nunataks, following a period of very rapid thinning, the ice sheet surface had lowered to its present elevation by the mid-Holocene (7.9 ka at Maish Nunatak and ~6 ka at Mt Moses). This finding is corroborated by a recently acquired suite of cosmogenic nuclide exposure ages from five additional nunataks, all situated adjacent to PIG (Nichols et al., 2023). Any record of late Holocene exposure at these sites – which would imply thinning below present elevation and grounding-line retreat inboard of its present position – must therefore currently lie beneath the ice sheet surface, making these nunataks potentially suitable locations for our study. Thus, based on knowledge of Holocene exposure history alone, subglacial drilling at any of Mt Moses, Shepherd Dome, Evans Knoll or Maish, Inman, Meyers and Winkie nunataks (Fig. 1b) would have the potential to reveal the late Holocene record of thinning in this region. The current lack of exposure histories from other peaks in the Hudson Mountains (for example, World's End Bluff and

Webber Nunatak) does not necessarily rule them out as suitable drill sites, assuming that the ice sheet behaved similarly around them also. We therefore sought other types of data to inform our drill site selection.

3.1.2 Nunatak topography

The relative suitability of Maish, Webber, Winkie, Meyers and Inman nunataks, World's End Bluff and Shepherd Dome (Fig. 1b) as drill sites can be further evaluated based on their present topographic shape. Prior to undertaking fieldwork, we used satellite imagery to assess this visually. Winkie and Meyers nunataks each comprise a single ridge, Webber Nunatak has two ridges extending towards Larter Glacier and Maish Nunatak has three ridges which extend inland (see Figs. 6, 10 and 14). In contrast, neither World's End Bluff, Shepherd Dome nor Inman Nunatak has any ridges. Inman Nunatak has a dome-like shape with outcrops largely across its northern flanks, World's End Bluff is a partially ice-covered flat-topped feature with a near-vertical cliff face extending towards the northern Pine Island Ice Shelf on its western side (Fig. 1b), and Shepherd Dome consists of an ice dome with a few small patches of outcrop on its southern side. Thus, these three sites are not as suitable for drilling as Maish, Webber, Winkie and Meyers nunataks.

3.1.3 Modelling

We used ice sheet model simulations to assess the sensitivity of ice cover to grounding-line retreat. This approach enabled us to consider where the grounding line would likely be situated relative to each nunatak during hypothetical periods of a smaller-than-present ice sheet, and to evaluate the orientation of individual ridges relative to the retreated grounding line. Subglacial bedrock that is most likely to yield evidence of ice sheet thinning and rethickening as a result of grounding-line retreat-readvance during the late Holocene will be located on the subglacial extensions of currently exposed ridges that extend perpendicular to the former grounding line (see section 2).

The Net Sum Model (NSM) simulations from Larour et al. (2019), run using the Ice Sheet System Model (Larour et al., 2012), are suitable for the present study because they i) use a relatively high resolution (1 km) over the Hudson Mountains and ii) can simulate future grounding line positions analogous to those we would expect during periods when the ice sheet was smaller. Figure 4 shows the modelled versus observed modern grounding line positions near PIG, and modelled position for the year 2350. As expected, the model does not do a perfect job in reproducing the observations. For example, it is not physically plausible that the grounding line is presently situated between Maish Nunatak and Mt Moses, as simulated (model GL 0 yr; Fig. 4). However, closer to PIG, and around Evans Knoll, the observed and modelled modern grounding line positions correspond relatively closely, giving confidence in the model's ability in that region. The simulation for model year 2350 shows a much-retreated grounding line in many parts of the Hudson Mountains, particularly in the main glacial troughs (e.g. Larter Glacier) where it is predicted to migrate several tens of kilometres upstream of present. We use this future simulation as an analogy for a hypothetical grounding-line retreat inboard of its present position (followed by a readvance).
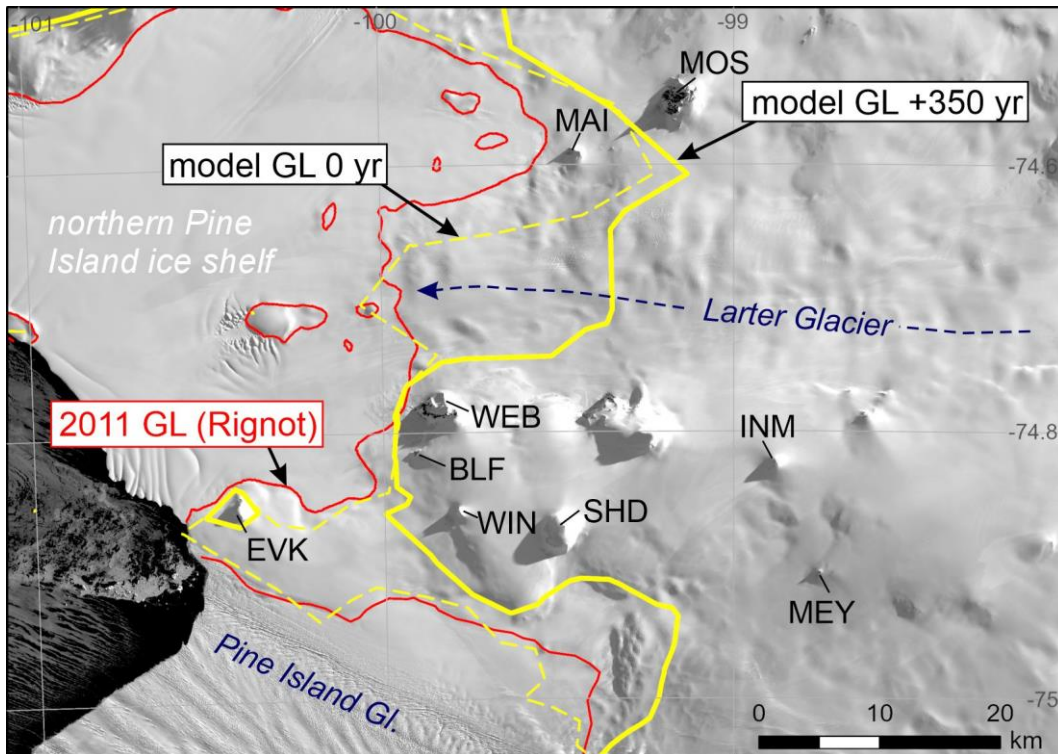
Figure 4: Position of present and modelled (future) grounding lines relative to nunataks in the Hudson Mountains region. The modern (2011) observed grounding line position is shown as a solid red medium-thickness line (Rignot et al., 2016). The modelled grounding line position at present-day (model GL 0 yr) is shown as a thin dashed yellow line, and at 350 years into the future (model year 2350) as a thick yellow line (model GL +350 yr). Both are from the NSM simulations of Larour et al. (2019). The underlying satellite image is Landsat-8, courtesy of USGS. Nunataks mentioned in the text are labelled as follows: EVK (Evans Knoll), BLF (World's End Bluff), WEB (Webber Nunatak), WIN (Winkie Nunatak), SHD (Shepherd Dome), INM (Inman Nunatak), MEY (Meyers Nunatak), MAI (Maish Nunatak), MOS (Mt Moses).

In the +350 yr future simulation (as well as in other future runs of Larour et al., 2019 not shown here), the modelled grounding line is retreated into the glacial troughs such that it passes within a few kilometres of some of the nunataks. In that situation, we would expect ice cover on N-S-oriented ridges of those nunataks to reduce as the grounding line retreated. For example, the +350 yr modelled grounding line position implies that ridges on the northern side of Webber Nunatak would be oriented perpendicular to it if the grounding line had retreated inboard of present (Fig. 4), making them potentially suitable sites from which to collect a transect of subglacial drill cores that could provide evidence of progressive late Holocene retreat. The model simulations also provide insight into what would become of Evans Knoll in a more retreated situation. At present, the grounding line skirts Evans Knoll on its western side, linking it to the mainland (Fig. 4). However, in the +350 yr model simulation, the knoll becomes an island rather than becoming more exposed. In that situation, since no additional bedrock is exposed during

240 retreat, records of late Holocene ice sheet change are unlikely to be found in the presently-subglacial bedrock, and the site would thus probably prove unsuitable for determining whether or not retreat inboard of present occurred.

Other models could be used to inform the selection of suitable subglacial drill sites. For example, models that predict ice sheet thickness changes through time may show which sites deglaciate the most during grounding-line retreat (e.g. the BISICLES

245 ice flow model; Nias et al., 2019). We chose to use a model that simulates future, rather than past, ice sheet configuration because (to our knowledge) no palaeo-ice sheet models have yet been able to simulate grounding-line retreat inboard of present in the Pine Island-Thwaites Glacier region under climatic and ocean forcing that would be considered realistic for the Holocene, and new modelling was beyond the scope of our study. However, such palaeo-ice sheet model outputs could be used for assessing drill site suitability if available in future. Nevertheless, the challenge with all models used for this purpose is that

250 they must be of sufficiently high spatial resolution to resolve small-scale ice sheet changes around nunataks that are often only a few kilometres apart (Mas e Braga et al., 2021). Continent-wide ice sheet models are currently not capable of this, and even with nested domains at higher resolution, it is challenging (Johnson et al., 2021). This situation is, however, likely to improve in the near future as models evolve. In summary, based on the model comparison described above, the most suitable drill sites in the Hudson Mountains are those that are (i) currently situated in close proximity to the modern grounding line and (ii)

255 unlikely to have become an island if the grounding line was situated inboard of its present location. They are Maish, Webber, and Winkie nunataks, World's End Bluff and Shepherd Dome (Fig. 4).

3.1.4 Bedrock lithology and structure

The lithology of the subglacial bedrock is important to know prior to drilling to ensure that enough of the target mineral can be collected for cosmogenic nuclide analysis (see section 2). Furthermore, to maximise the chance of successful core recovery,

260 the bedrock structure − specifically permeability and consolidation − must be known. Although there is very little published information about the geology of the Hudson Mountains, they are known to be volcanic. Several are basaltic and contain olivine and feldspar phenocrysts (Rowley et al., 1990) making them potentially suitable for cosmogenic nuclide analysis, including in situ ^{14}C. Of the candidate drill sites, Webber Nunatak and Shepherd Dome consist of basaltic lava flows and hyaloclastite tuff, World's End Bluff is composed entirely of hyaloclastite tuff, and Maish Nunatak consists of subaerial

265 basaltic lavas (Lopatin & Polyakov, 1974; Rowley et al., 1990). In contrast, the lithology of Winkie Nunatak (basaltic lava; section 3.2.1) was unknown prior to our field survey. "Hyaloclastite" is used in this paper to include all hydroclastic fragmental rocks including hyaloclastite (*sensu stricto*), tuffs and lapilli tuffs, regardless of the specific mode of fragmentation (cf. White & Houghton, 2006).

270 Both basalt and hyaloclastite can be cored with typical rock drilling systems if joints and fractures in the rock are filled with ice. This has been the case in all previous Antarctic subglacial drilling campaigns and is likely in the Hudson Mountains since the candidate drill sites are all relatively low elevation (< 550 m asl) and experience melting at the ice margin as a result of

solar heating during the austral summer. However, a weakly consolidated hyaloclastite could create several potential problems with core recovery, including core fragmentation, core loss during break-off, or loss of unconsolidated clay or fines to the

275 drilling fluid (particularly a problem for hyaloclastite which is typically rich in palagonite, a mixture of clay minerals; Stroncik & Schmincke, 2002). A well consolidated crystalline basalt, even if vesicular, will most likely yield a higher-quality and more complete core. Thus, from the perspective of bedrock lithology and structure alone, Maish Nunatak, Webber Nunatak, World's End Bluff and Shepherd Dome are probably plausible for successful drilling and core recovery, and depending on the results of our field survey, Winkie Nunatak may be also (Shepherd Dome and World's End Bluff were, however, discounted based

280 on their unsuitable topography; section 3.1.2).

3.1.5 Summary

The results of the surveys we undertook prior to fieldwork provided an initial assessment of sites that could be suitable for drilling and warranted further investigation. Sites where ridges are not present (World's End Bluff, Inman Nunatak and Shepherd Dome) did not pass this initial filter and were excluded from further investigation. Sites that passed, or based on the

285 available data could not definitely be ruled out as unsuitable, are listed in Table 1. We subsequently assessed these in detail through comparison with the model outputs and via ground-based field survey. Since two of the sites that passed the initial filter (Evans Knoll and Meyers Nunatak) appear from comparison with modelling not to be sensitive to PIG grounding line migration, we concluded that drilling into subglacial bedrock close to one or more of Winkie Nunatak, Webber Nunatak and Maish Nunatak would provide the best chance of obtaining evidence for/against a smaller ice sheet in the late Holocene in the

290 eastern Pine Island-Thwaites Glacier system. Our reconnaissance field survey therefore focused on these three sites.

Site name	Latitude (DD)	Longitude (DD)	Ridges present?	Sensitive to PIG grounding line migration?	Suitable bedrock lithology?*	Drill site safely accessible?*	Quartz-bearing erratics present?*
Winkie Nunatak	-74.86	-99.77	✓	✓	✓	✓	✓
Webber Nunatak	-74.77	-99.83	✓	(✓)	(✓)	✓	✓
Evans Knoll	-74.85	-100.41	(✓)	(x)	✓	✓	✓
Meyers Nunatak	-74.91	-98.75	✓	x	(x)	N/A	N/A
Maish Nunatak	-74.60	-99.34	✓	✓	✓	(x)	✓

Table 1: Suitability of sites in the Hudson Mountains for subglacial bedrock drilling. Each site with ridges present was then assessed against the key criteria shown in the subsequent column headings. Asterisks indicate criteria that require field survey for full assessment.
295 Key: ✓ = yes; (✓) = probably, but with some challenges/caveats; (x) = unclear/probably not (or at least not without major challenges or uncertainty); x = no; N/A = not applicable because site is ruled out based on other criteria.

3.2 Field survey of candidate drill sites in the Hudson Mountains

We conducted a ground-based survey of the Hudson Mountains in the austral summer of 2019-20, using the criteria outlined
in section 2 to establish the suitability for drilling of the three candidate drill sites, Winkie Nunatak, Webber Nunatak and
Maish Nunatak. The results of our field survey (geological and glaciological observations, and sub-ice features from GPR
surveys) are described here and summarised in Table 1. The bedrock lithology at each site was studied in detail following the
fieldwork, using rock samples collected from the ridges. Details of the radar survey methods are provided in Appendix A.

3.2.1 Winkie Nunatak

Winkie Nunatak (Fig. 5) is a ridge rising 110 m above the ice sheet surface that is composed entirely of basaltic pillow lavas,
overlain by numerous granite erratics. The ridge is broadly oriented N-S and dips perpendicular towards PIG (Fig. 1), making
it highly likely to have been more exposed during any periods when the grounding line was retreated relative to present. The
exposed part of the ridge is broad and rounded, with a gentle gradient (Fig. 5a).
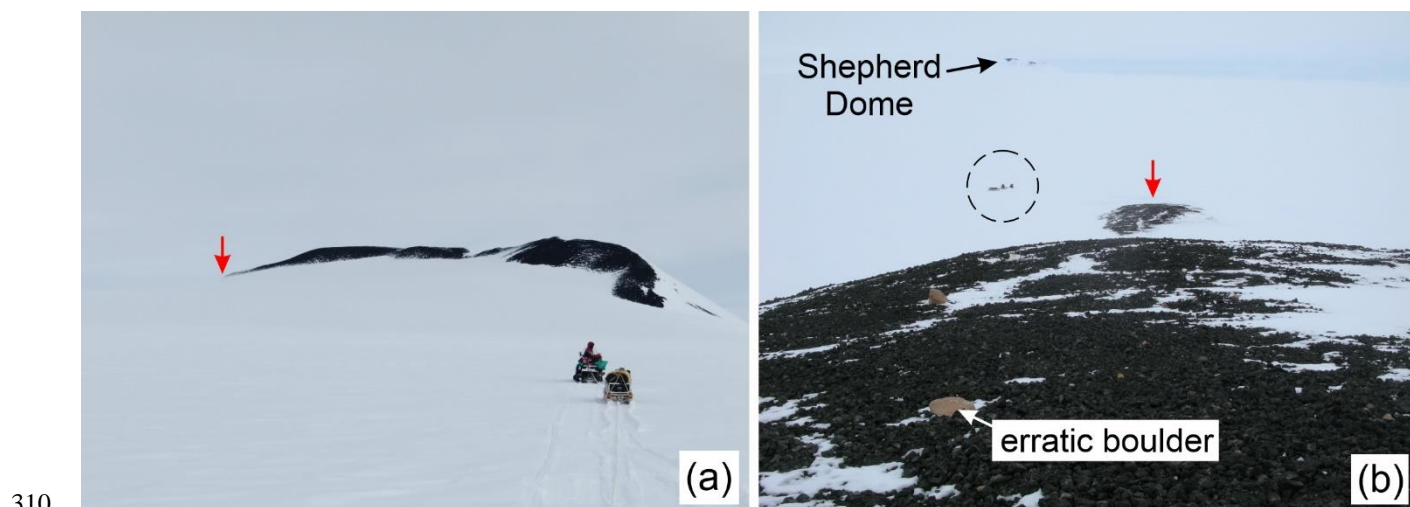
Figure 5: Topography and surroundings of Winkie Nunatak. **(a)** Winkie Nunatak viewed from the north. Arrow indicates where the SE
ridge extends below the ice surface. Sledge and snowmobile for scale. **(b)** View looking down the SE ridge towards Shepherd Dome. Red
down-pointing arrow shows tip of ridge. Note glacial erratics strewn on lava bedrock surface. Sledge and two snowmobiles (circled) for
scale.

Accessibility: Although there is heavy crevassing on the western side of Winkie Nunatak and to the south (Fig. 6), safe access
to the base of the ridge at its SE end was possible at the time of our survey by approaching the nunatak from the NE. The area
between Winkie Nunatak and Webber Nunatak is several kilometres wide and relatively flat, enabling the required access by
ski-equipped aircraft (see section 2). A skiway at this location would allow a camp to be situated within 5 km of the base of
Winkie Nunatak, allowing for fast and safe transit between the camp and drill site for the drilling team.
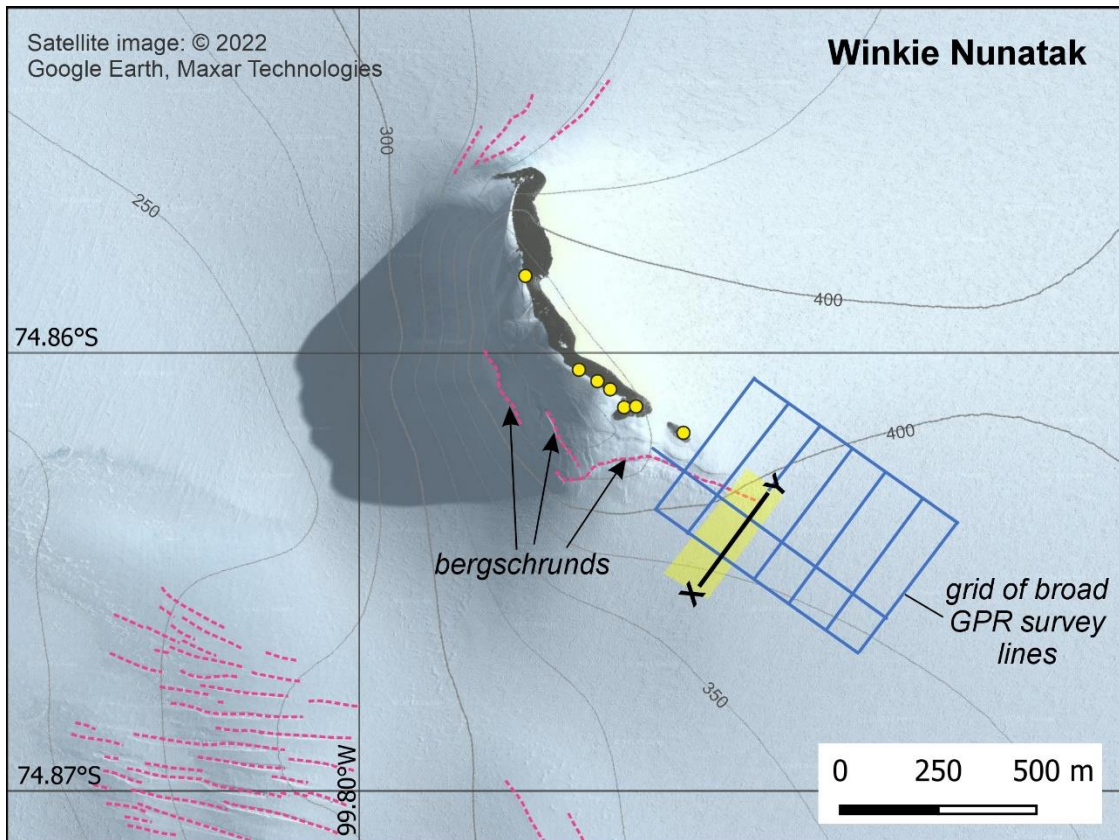
Figure 6: Satellite image of Winkie Nunatak, showing areas of known crevassing (pink dotted lines). Contours of surface elevation (at 25 m intervals) are from the REMA DEM (Howat et al., 2022). Satellite image ©2022 Google Earth, Maxar Technologies (imagery date: 16 February 2012). Locations of glacial erratics dated by Nichols et al. (2023) are indicated by yellow circles. The location of radar profile (X-Y) in Fig. 8 is shown here inside a shaded yellow rectangle that outlines the coverage of our detailed survey grid (five lines; see Appendix A). The lines of the broader GPR survey (Appendix A) are also shown.

Bedrock lithology: Winkie Nunatak is comprised entirely of pillow basalt lavas that contain abundant unweathered olivine and plagioclase feldspars − but no pyroxene − in a fine-grained matrix (Fig. 7a and b). Using a thin section of a sample taken from the central crystalline core of a pillow during the field survey (Fig. 7b and c), we measured the olivine crystals as 0.1-1.5 mm in diameter and plagioclase laths as 0.2-0.9 mm in length. We visually estimated their abundances as 10-15 % (olivine) and 20-25 % (feldspar). The phenocrysts are present, but less abundant, in the vesicular outer pillow rims. Due to their relatively large size, the olivines – and to a lesser extent the feldspars − would be straightforward to mechanically separate (using magnetic and density separation). Thus, although the bedrock at Winkie Nunatak does not contain the most desirable mineral phase for [10]Be and in situ ^{14}C cosmogenic nuclide measurements (quartz), the presence of separatable olivine should make in situ ^{14}C dating feasible (see section 2).
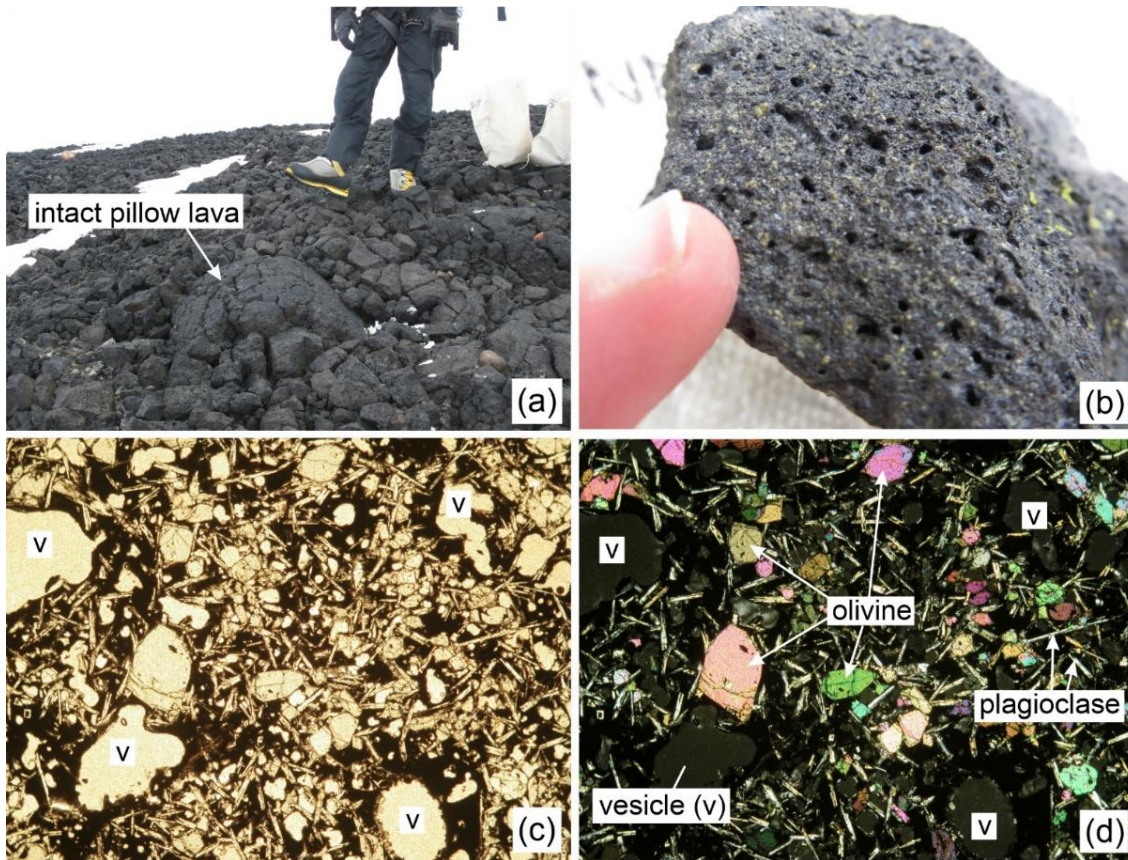
340 **Figure 7: Photographs showing bedrock lithology at Winkie Nunatak.** **(a)** Field photograph of pillow basalt. Person for scale. **(b)** Close-up photograph of lava, showing abundant olivine phenocrysts (green crystals). Fingertip for scale. **(c)** Thin section of lava (sample UNN-204; British Antarctic Survey ID R19.1.12), shown in Plane Polarised Light (PPL). Field of view is 8 mm. **(d)** Thin section of same lava and same field of view as in panel c, shown between crossed polars (XPL). Field of view is 8 mm. v=vesicle (hole created by gas or steam during rock solidification after eruption)

345

Glaciology: The ice sheet surface surrounding Winkie Nunatak consists of well-compacted firn covered by snow, with small sastrugi (< 30 cm high) covering most of the snow surface in the 2019-20 season. The ice surface slopes gently away to the SE from the end of the main ridge of Winkie Nunatak. Perpendicular to the ridge line, the ice slopes more steeply from the north towards the margin of PIG. A few large crevasses and a bergschrund are visible in satellite imagery (Fig. 6) and were

350 also observed during fieldwork. Although well-bridged in 2019-20, these crevasses could limit or prevent future access from both the northern end of the ridge and its SW side. The GPR survey also showed some large crevasses running away from the exposed bedrock ridge, parallel to the crest of convexity in the ice surface. Subsequent surveys in 2022-23 (Braddock et al., 2024) revealed multiple additional large extensional crevasses, covered only by thin (0.5 m-thick) snow bridges, running at oblique angles over the subglacial extension of the main ridge. These new shallow crevasses are likely a result of the rapidly

355 changing grounding line and ice margin position of PIG: the floating ice margin retreated past Winkie Nunatak between the 2019-20 season and the 2022-23 season as large icebergs calved from the terminus of the glacier (Joughin et al., 2021). Several similar calving events have been observed in the past decades (Jeong et al., 2016; Arndt et al., 2018).

Results of the GPR survey at Winkie Nunatak are shown in Fig. 8. The basal reflector indicates a well-defined ridge running
360 out in line with the exposed ridge of Winkie Nunatak and dipping quickly to 60 m beneath the ice surface at the centre of the detailed grid shown in Fig. 6, 210 m from the lowest bedrock exposure (position marked by the down-pointing red arrow in Fig. 5b). Below the ice surface, the ridge crest gradually flattens, reaching a width of 20-30 m and widening further as it deepens towards the SE (Fig. 8c). The subglacial ridge is covered by well compacted firn (with continuous layers clearly visible; Fig. 8b), likely transitioning to ice at depth. There are, however, two large, buried crevasses marking the extension of
365 the bergschrunds that run across the south-facing slope of the nunatak (Fig. 6). Offline reflectors from the ridge obscure some lower internal ice reflectors, making it difficult to identify any near-bedrock layering in the ice column or at the ice-bedrock transition.

Our GPR observations suggest that, from a glaciological point of view, the subglacial ridge extending SE towards PIG is an
370 ideal drill site for drilling. The ridge crest is wide and continues as a discrete ridge for over 300 m before it dips to an ice depth of >100 m. The centre of the ridge should thus be accessible for much of its length and the large, buried crevasses on its crest can likely be avoided (or drilling away from the ridge crest could be considered). The continued dip below the ice surface of the exposed bedrock at the SE end of Winkie Nunatak suggests that the exposed bedrock is likely to be representative of the subglacial extension of the ridge.

375
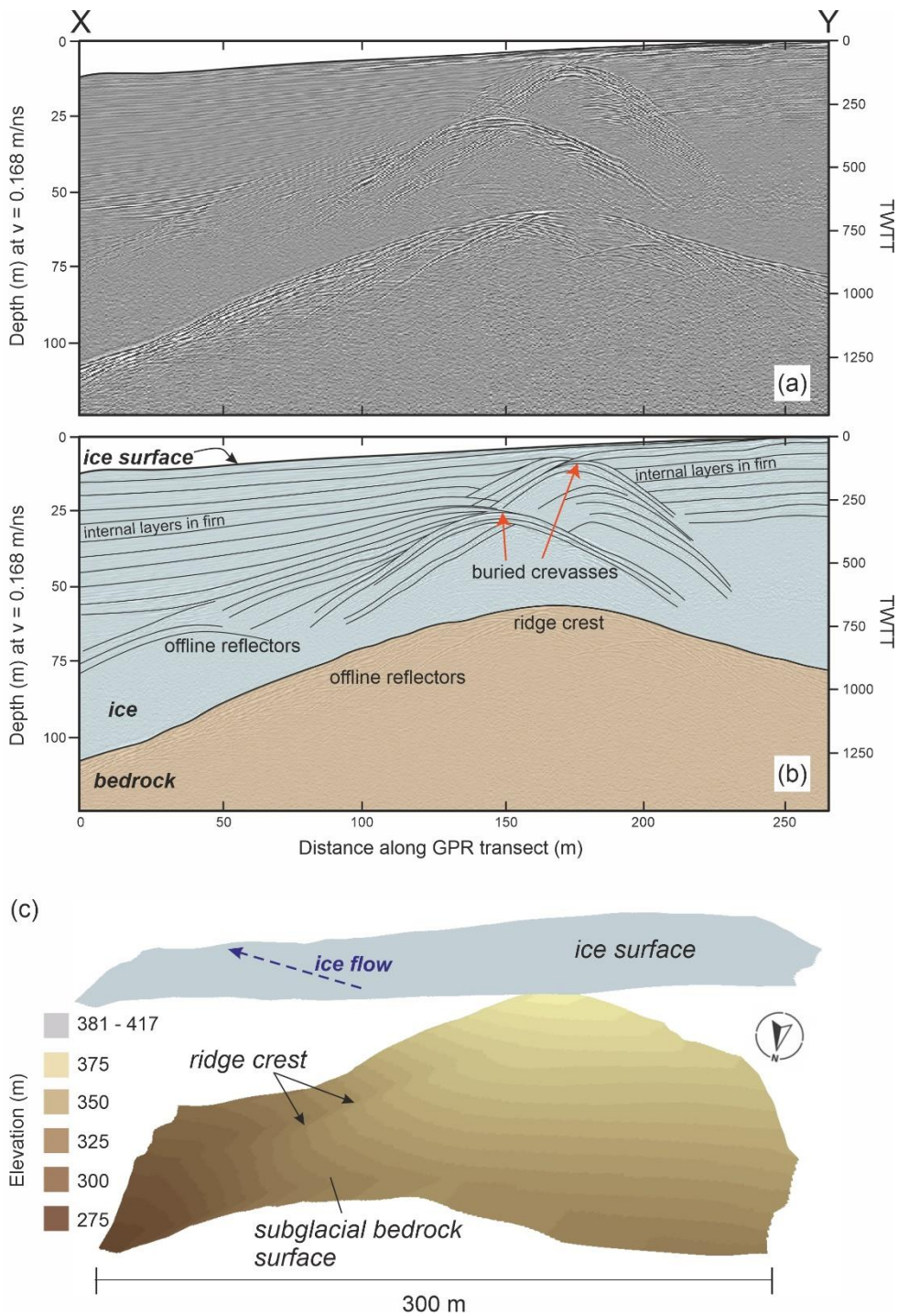
Figure 8. GPR survey results from Winkie Nunatak. (a) 2D radar profile (the location of profile X-Y is shown in Fig. 6). TWTT is two-way travel time. **(b)** 2D radar profile showing digitised basal topography and ice. Subsurface features including firn layers, crevasses and offline reflectors from basal bedrock are labelled. **(c)** Radar-based interpolation of the subglacial bedrock ridge (the area covered by these data is shown in Fig. 6).

3.2.2 Webber Nunatak

Webber Nunatak (Fig. 9) is an eroded volcanic edifice situated adjacent to Larter Glacier (Fig. 1). Modelling suggests that, if the grounding line had ever retreated inboard of its present position, it would likely have retreated up the Larter Glacier trough (Fig. 4). Two prominent ridges extending down to Larter Glacier on its northern side (Fig. 9a) are oriented perpendicular to that trough, making them sensitive to ice sheet thickness changes resulting from grounding-line retreat; from this perspective, they make suitable drill sites. One of the ridges ('Ridge A'; Fig. 9a) descends relatively gently to a blue ice area where katabatic winds scour snow away from the ice surface, another feature that makes Ridge A suitable for drilling (section 2 and caption to Fig. 3). The nunatak is composed of a sequence of lavas and stratified hyaloclastite, but in contrast to Winkie Nunatak, only a handful of erratic cobbles and boulders are present; most are quartz-bearing granitoids with a few gneisses (Fig. 9d), making them ideal for cosmogenic nuclide dating to determine the past exposure history of the ridge. Although erratics are only present on the lowermost 70 m of the two ridges, and predominantly on Ridge A, this should not present a problem for detecting Holocene retreat-readvance because only erratics from close to the modern ice surface are needed to provide a constraint on the exposure history of the subglacial portion of the ridge (Johnson et al., 2022).
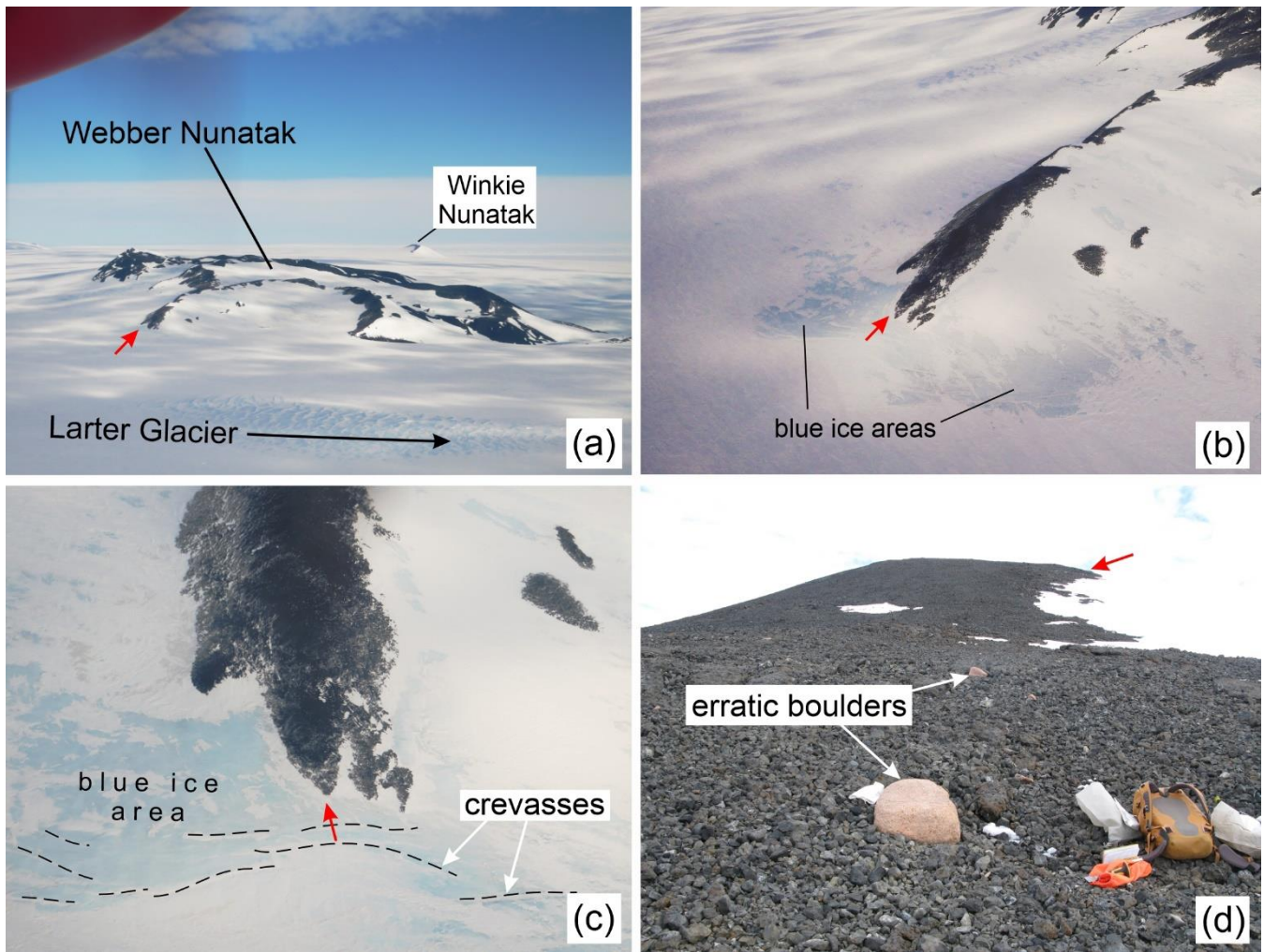
Figure 9. Topography and glaciology around Webber Nunatak. Short red arrows denote 'Ridge A' (see text). **(a)** Webber Nunatak viewed from Larter Glacier, showing candidate drill site (off end of Ridge A). Note extensive crevassing on Larter Glacier, preventing access by aircraft from the northern side. The nunatak length from left to right in the image is 3.5 km. **(b)** Ridge A (width ~150 m) viewed from the air. **(c)** Close-up view of ridge A (width ~150 m) and the adjacent blue ice area, viewed from above. Several crevasses are visible extending perpendicular to the ridge. **(d)** The lower part of Ridge A, looking towards Larter Glacier. A few erratics are perched on the basalt rubble. Rucksack and field equipment for scale; the boulder in the foreground is 50 cm diameter.

400
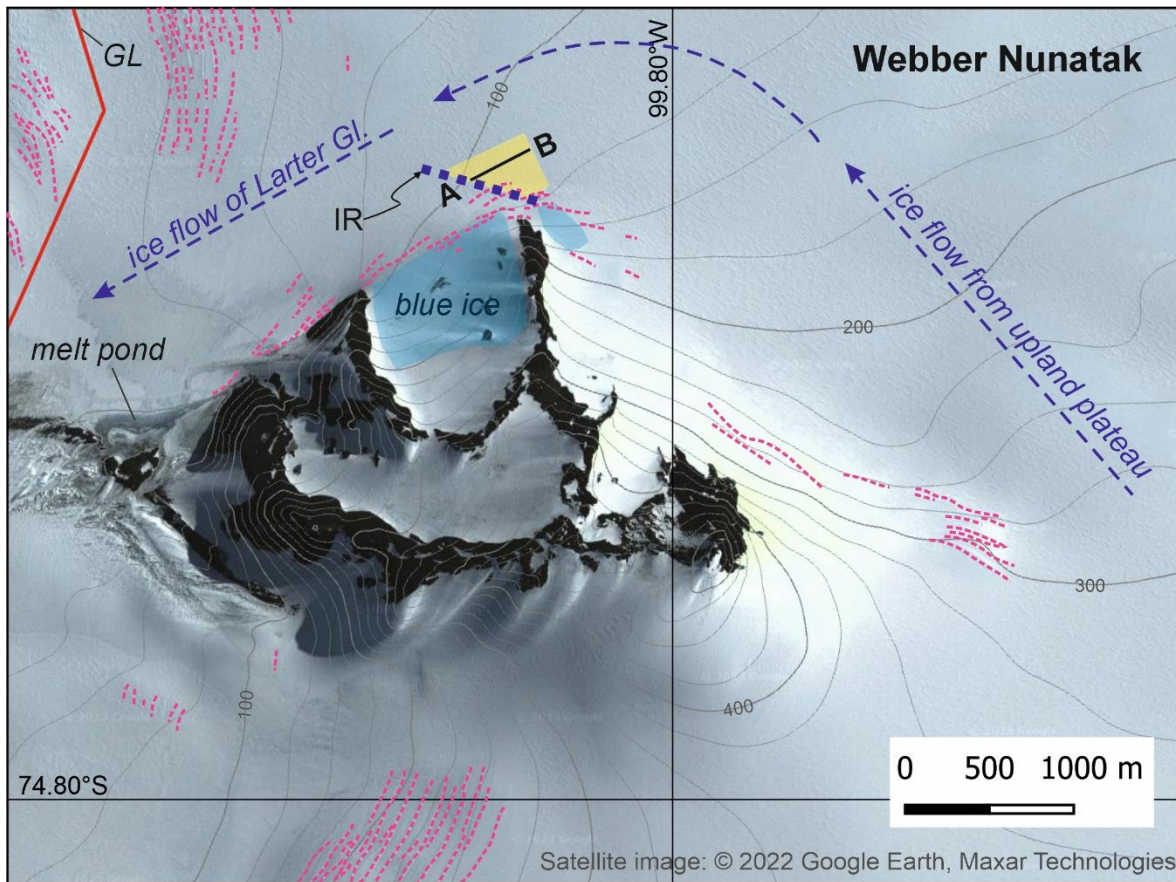
Figure 10. Satellite image of Webber Nunatak, showing areas of known crevassing and blue ice. Pink dotted lines and blue shaded areas show location of crevasses and blue ice, respectively. The location of the radar profile (A-B) shown in Fig. 12a and b is indicated by a shaded yellow box that outlines the survey area used to compile Fig. 12c. The dotted line labelled 'IR' shows the base of a ridge in the ice sheet surface. Numerous large crevasses were observed on the ridge slope to the SW of the line. Contours of surface elevation (at 25 m intervals) are from the REMA DEM (Howat et al., 2022). The solid red line (labelled 'GL') marks the location of the 2011 grounding line (Rignot et al., 2016). Satellite image ©2022 Google Earth, Maxar Technologies (imagery date: 16 February 2012).

Accessibility: In contrast to Winkie Nunatak, access to Webber Nunatak is more challenging due to the presence of several large crevasses close to its eastern end (Fig. 10). Furthermore, the downstream section of Larter Glacier on the northern side of Webber Nunatak is heavily crevassed making it impossible to land an aircraft there (Fig. 9a). The only way to access a drill site at the base of the ridges on the northern side of Webber Nunatak would be from a camp situated in the broad flat area between Winkie Nunatak and Webber Nunatak (Fig. 1b). The crevassing could then be avoided by driving in a wide berth around the eastern end of Webber Nunatak. Whilst feasible, this adds time for driving a few extra kilometres from the camp to the work area, but it would be impossible to bring the drill and associated equipment to the foot of those ridges by any other route. The work area at Webber Nunatak is also limited to a footprint extending up to ~800 m from the northern ridges, due to the proximity to the shear zone of Larter Glacier (Fig. 9a). Care would also be needed to avoid smaller crevasses perpendicular

to the base of those ridges (Figs. 9c and 10); it may alternatively be possible to bridge the crevasses using aluminium ladders to permit safe rope-free access to the drill site. These aspects mean that ridges on the northern side of Webber Nunatak could be workable, but access would not be as easy or as safe as at Winkie Nunatak.

425
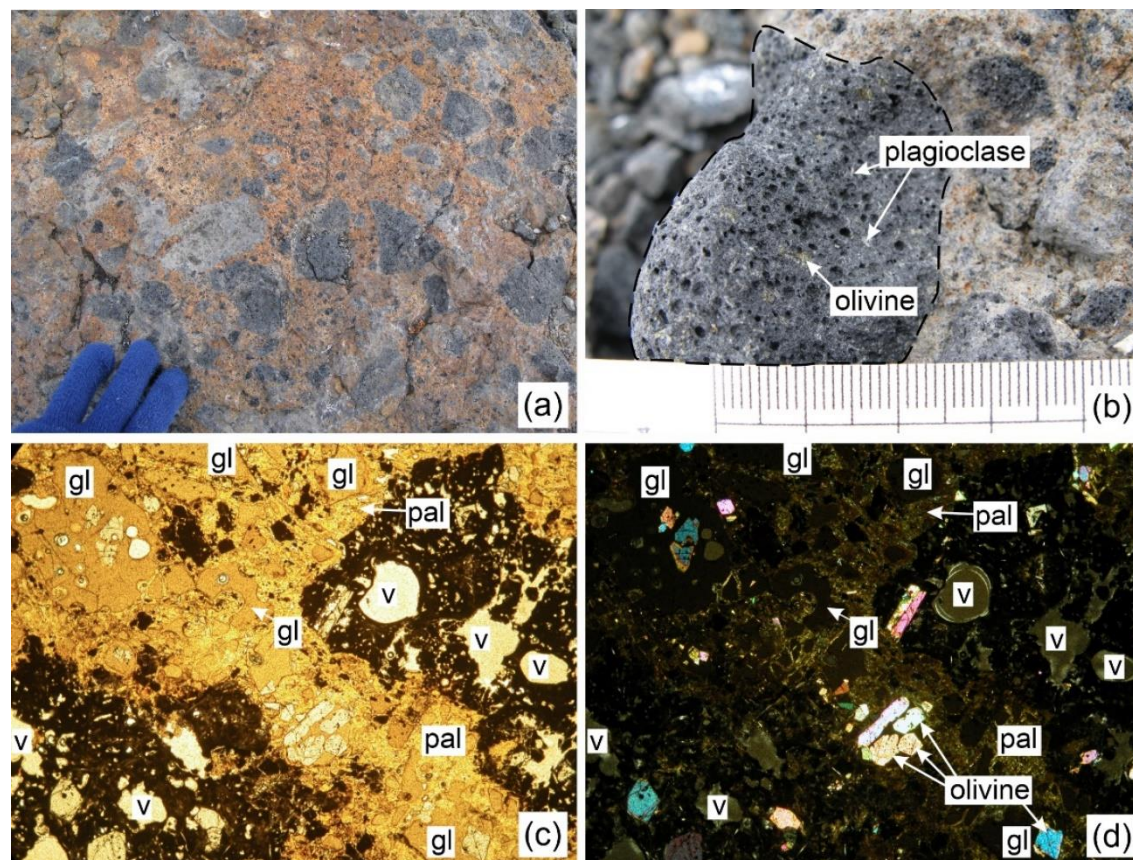
Figure 11. Photographs showing bedrock lithology at Webber Nunatak. (a) Field photograph of hyaloclastite at Webber Nunatak, from the base of a ridge that extends towards Larter Glacier close to a potential drill site. Large basalt clasts (grey) are surrounded by palagonitised glass matrix (orange). Gloved hand for scale. **(b)** Close-up field photograph of Webber Nunatak hyaloclastite, showing basalt clast (outlined by dashed line) containing abundant olivine and plagioclase phenocrysts. Scale bar increments are in mm. **(c)** Thin section photograph of
430   hyaloclastite (sample WEB-211; British Antarctic Survey ID R19.2.11) in PPL. Field of view is 8 mm. v=vesicle, gl=glass (orange colour), pal=palagonite (yellow colour) **(d)** Thin section photograph of same hyaloclastite and same field of view as in panel c, in XPL. Field of view is 8 mm. v=vesicle, gl=glass (in extinction), pal=palagonite (birefringent)

Bedrock lithology: The lower ridges on the northern side of Webber Nunatak consist of massive (unstratified) hyaloclastite
435   (Fig. 11). Some of the glass within the hyaloclastite has been converted to clay minerals, specifically palagonite, by alteration (Fig. 11c; cf. fig. 4, Johnson & Smellie, 2007). Interspersed with the glass are clasts (typically <6 cm diameter) of basaltic lava that contain abundant olivine phenocrysts of 0.2-1.0 mm diameter (Fig. 11b) but no visible pyroxene or feldspar. Presence of these lava clasts in any recovered drill core would allow measurement of cosmogenic ^{10}Be and in situ ^{14}C in olivine (see section

2), but such analyses would be dependent on recovering enough material: since the diameter of rock cores is typically only 2-5 cm, there would be a high likelihood of penetrating only (or predominantly) the glassy material that would be unsuitable for cosmogenic nuclide analysis. Thus, although it would theoretically be possible to measure cosmogenic nuclides in the Webber Nunatak bedrock, it would probably be extremely challenging, and potentially impossible.

Glaciology: The ice sheet surface at the base of Ridge A consists largely of blue ice with some firn, and patchy snow cover (Fig. 9). Numerous crevasses are present around the base of the ridge (Fig. 10). Some are >1 m wide and are filled with aerated unconsolidated snow and ice. We estimated they could be >2 m deep. During the 2019-20 season, the snow bridges of these crevasses were weak, likely due to the warm temperatures experienced in late 2019. The ice surface showed two elevations, with a higher (heavily crevassed) area and a lower, flatter area to the east. A steep slope separated the two areas, again with numerous crevasses, with the base of the slope trending NW from the end of the bedrock ridge. The results of our GPR survey at Webber Nunatak (Fig. 12) indicate that the main subglacial bedrock ridge trends to the NW, with the highly crevassed ice ridge marking its crest. It is fairly broad – rounded, rather than sharp-crested − beneath the ice surface (Fig. 12c). The bedrock ridge also appears to have been heavily eroded by ice moving NW from the plateau ice between Webber Nunatak, Mount Manthe and Shepherd Dome (Fig. 1b), before meeting Larter Glacier ice flowing WSW. There are few clearly discernible structures visible within the ice in the GPR data. Near the surface, a firn layer that extends to ~50 m below the modern ice sheet surface can be traced in places, and some offline bedrock reflectors are also apparent (Fig. 12a and b).

In summary, GPR and glaciological field observations suggest that drilling at the end of Ridge A at Webber Nunatak would be challenging due to the presence of large poorly bridged crevasses around the base of the exposed ridge. These would make access difficult, as well as reducing the options for recovering a closely spaced transect of subglacial bedrock cores.
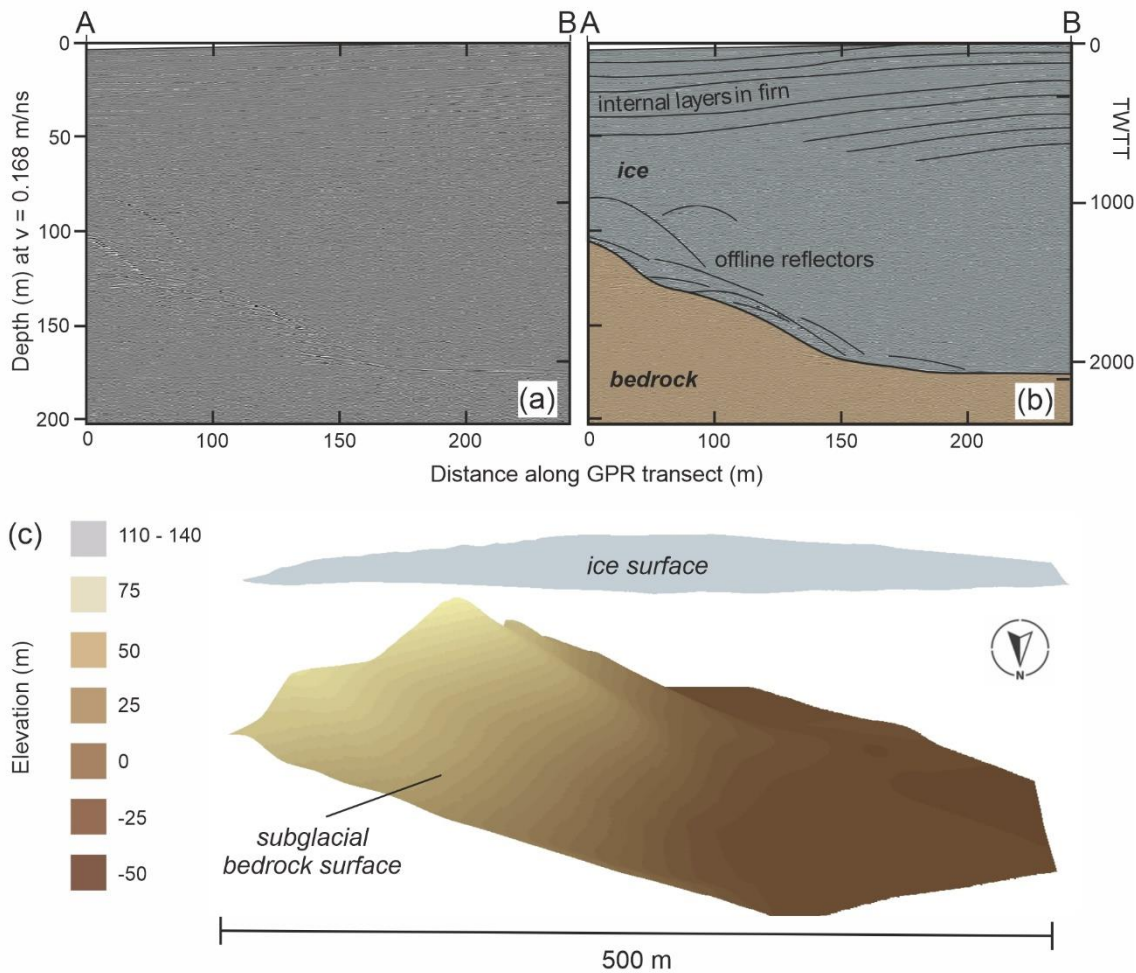
Figure 12. GPR analysis of Webber Nunatak. (a) and **(b)** 2D radar profile, showing subglacial ridge crest (location of profile A-B is shown in Fig. 10). TWTT is two-way travel time. Panel (b) shows digitised basal topography and the ice surface and is annotated to show subsurface features (thin black lines). **(c)** Radar-based interpolation of the subglacial ridge.

465

3.2.3 Maish Nunatak

Maish Nunatak is situated on the northern side of Larter Glacier, ~3 km from the modern grounding line (Fig. 1b). Its bedrock is composed entirely of basaltic pillow lavas. Granite erratics perched on the bedrock surfaces are much more numerous than at Winkie or Webber nunataks. Cosmogenic nuclide exposure dating of a suite of these erratics (locations shown in Fig. 13b)

470 showed that Maish Nunatak deglaciated rapidly in the early Holocene and that the modern ice surface elevation was reached by ~8 ka (Johnson et al., 2014). Maish Nunatak has three ridges facing SE that are very low gradient (nearly horizontal) on their ice-proximal ends (Fig. 13). Their orientation is not perfect for detecting past changes in grounding line position because they slope inland away from the modern grounding line and are protected by the higher elevation summit of the nunatak that

lies on the side closest to the grounding line. Nevertheless, existing exposure ages from the outermost ridges appear to have
475   captured ice sheet thinning that reached the modern surface elevation in the early Holocene. Thus, drilling at this site should
permit detection of Holocene grounding-line retreat-readvance if it occurred.
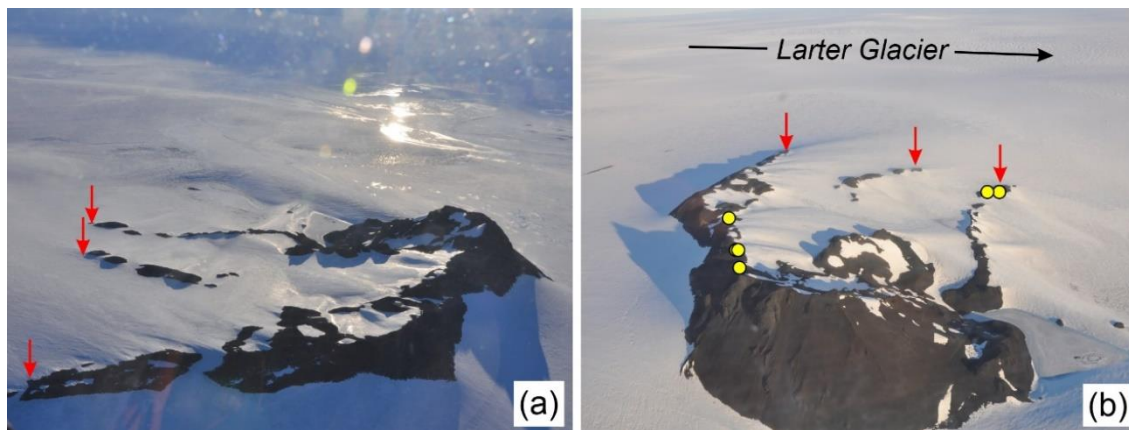
Figure 13. Topography and surroundings of Maish Nunatak. (a) View from the air, looking SW. Arrows indicate the tips of three low-
480   gradient bedrock ridges described in the text; the distance between the outer ridges is 880 m. **(b)** View looking approximately SE, towards
Larter Glacier. Circular symbols indicate the locations of erratic cobbles and boulders sampled for ^{10}Be exposure dating in an earlier study
(Johnson et al., 2014). As in panel (a), the outermost ridges are separated by a distance of 880 m. Both photographs were taken in 2010 by
James Smith (British Antarctic Survey).

485   **Accessibility:** There is very little crevassing visible from the ground or in satellite imagery in the immediate vicinity of Maish
Nunatak (Fig. 14). However, despite this and its suitability for drilling based on the surveys undertaken prior to fieldwork
(proximity to the grounding line, three ridges with a low gradient and well-constrained early Holocene exposure history), our
visit highlighted considerable challenges for access by a drilling team. Firstly, the nearest accessible location for ski-equipped
aircraft is on the SE side of Mt Moses, approximately 10 km from the ridges at Maish Nunatak (Fig. 1b). This would mean a
490   long travel time (>1 hour by snowmobile) from the landing site to the nunatak itself. In addition, the area between Mt Moses
and Maish Nunatak is an active ablation zone, where the presence of abundant tephras within the ice has resulted in differential
melting producing an extensive area of deep potholes within the ice surface (labelled 'zone of extensive surface melting' in
Fig. 14). Many of these metre-sized depressions of >50 cm depth were filled with slush during our visit. During warmer austral
summers, such slush/water-filled depressions could persist, causing the area to easily become completely impassable on foot
495   or by snowmobile. Therefore, the only plausible means for a drilling team and equipment to access Maish Nunatak is by
helicopter, establishing a camp on one of the lower rocky outcrops of the nunatak. For most Antarctic field campaigns,
helicopter support at this distance from an established base is unlikely to be a viable option. Thus, the difficulties of access are
a major shortcoming for Maish Nunatak as a potential drill site.
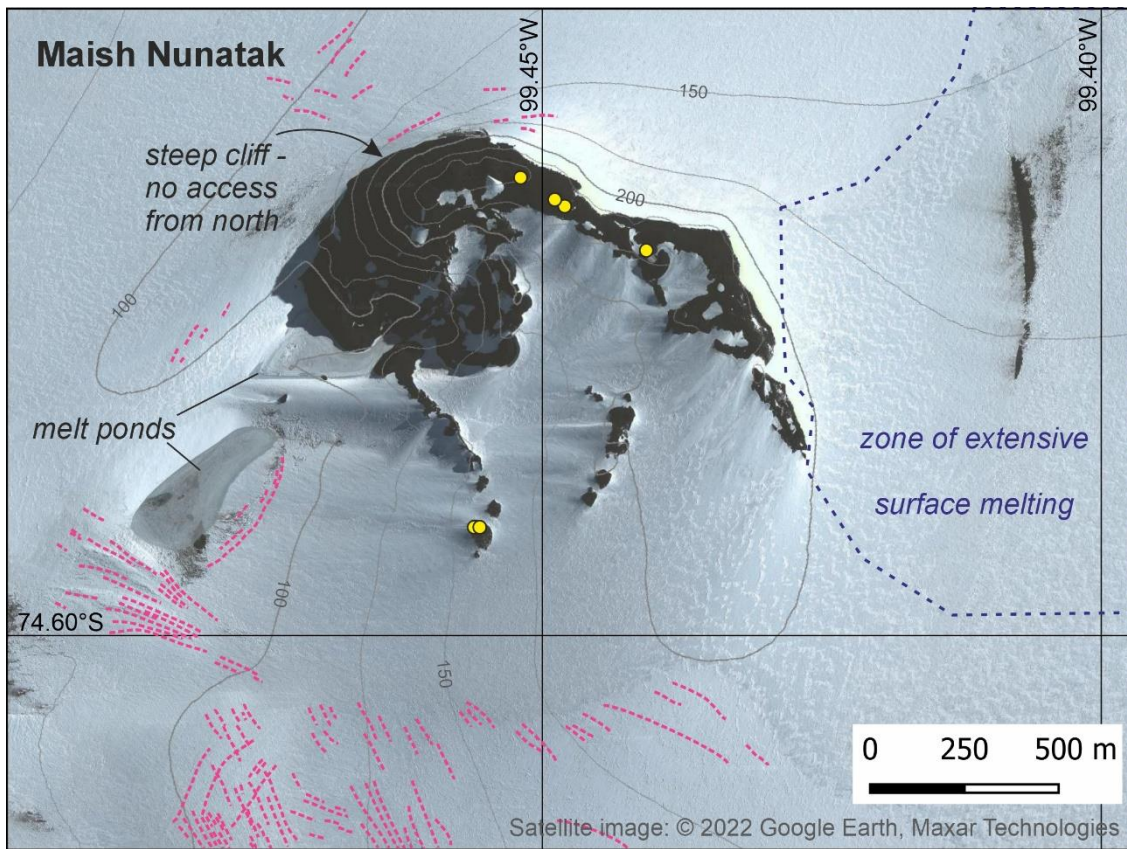
Figure 14. Satellite image of Maish Nunatak showing features that are important for drill site accessibility. Pink dotted lines show location of crevasses. Locations of erratic cobbles and boulders dated by Johnson et al. (2014) are indicated by yellow circles (see also Fig. 13b). No GPR surveys were undertaken at this site. Contours of surface elevation (at 25 m intervals) are from the REMA DEM (Howat et al., 2022). Satellite image ©2022 Google Earth, Maxar Technologies (imagery date: 2 March 2012).

Bedrock lithology: The bedrock lithology of Maish Nunatak is, however, relatively favourable for this study. It consists of basaltic pillow lava containing abundant fresh olivine phenocrysts, often clustered with plagioclase feldspar and occasional clinopyroxene, in a groundmass of fine-grained feldspar and clinopyroxene (Fig. 15 a and b). The olivine, clinopyroxene and feldspar phenocrysts are typically 0.25-1.25 mm, 0.25-0.4 mm and 0.5-1.25 mm diameter, respectively (Fig. 15c and d), making them relatively easy to separate from the groundmass. However, given their low overall abundance (<<5 %), the pyroxenes are unlikely to make suitable targets for cosmogenic nuclide measurement. This lithology is equally suitable for cosmogenic nuclide measurement as the Winkie Nunatak bedrock.
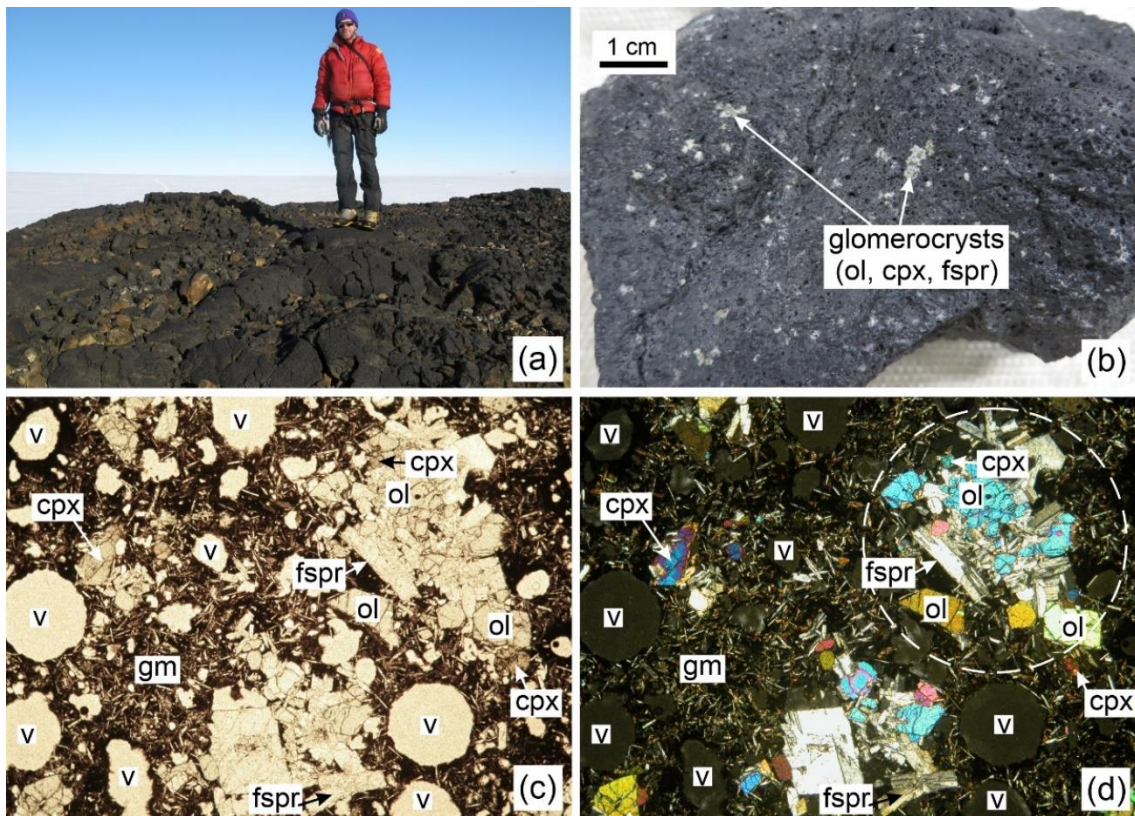
Figure 15. Photographs showing bedrock lithology at Maish Nunatak. (a) Field photograph of pillow lavas, with person for scale. **(b)** Close-up photograph of lava in hand specimen, showing prominent clusters (glomerocrysts) of olivine (ol), clinopyroxene (cpx) and feldspar (fspr). **(c)** Thin section photograph of lava (sample MAI-201; British Antarctic Survey ID R19.6.1), in PPL. Field of view is 8 mm. v=vesicle, gm=groundmass, cpx=clinopyroxene, ol=olivine, fspr=feldspar. **(d)** Thin section photograph of same lava as in panel c, in XPL. A glomerocryst is enclosed by the dashed white line. Field of view is 8 mm. v=vesicle, gm=groundmass (comprising feldspar and clinopyroxene crystals)

Glaciology: The ice sheet surfaces at Maish Nunatak consist predominantly of firn. We did not observe crevassing proximal to the three south-facing bedrock ridges (Fig. 13), an observation which is consistent with the generally low-gradient ice surface slopes around the nunatak. However, the ice surface at the base of the most easterly of the three exposed bedrock ridges has a reverse slope, and there are several small bedrock outcrops visible beyond the end of the exposed portion of the middle ridge. Together, these observations suggest that sections of these ridges dip below the ice surface and re-emerge further along, rather than sloping continuously away from the main outcrop. The exposed bedrock surface of the westernmost of the three ridges is slightly steeper than the other two, suggesting that its subglacial extension may also be steeper, although this is unlikely to pose difficulties for drilling. Although we were able to access Maish Nunatak in the 2019-20 season and assess some aspects of site suitability, GPR surveys were not undertaken there due to the challenges of towing equipment across areas of extensive surface melting (Fig. 14). The underlying ice structure and subglacial bedrock topography therefore remain unknown.

3.3 Final selection of drill site

Prior to field survey, we rejected Evans Knoll, World's End Bluff, Shepherd Dome, and Meyers and Inman nunataks as unsuitable for subglacial bedrock drilling aimed at detecting Holocene retreat-readvance. The decision over which of the remaining three potential drill sites (Winkie, Webber and Maish nunataks) is most suitable requires balancing of the relative importance of each of the criteria in Table 1. Whereas the suitability of the rock type for analysis and safe access for a field team are essential, there are trade-offs between ease of accessibility and likely ease of drilling/rock recovery (Briner et al., 2022); the latter will determine the speed at which samples can be collected (Braddock et al., 2024).

Based on lithological considerations alone, the most suitable bedrock for drilling is the basaltic lava at Winkie and Maish nunataks. In theory, it would be possible to recover and analyse the hyaloclastite bedrock at Webber Nunatak, but it would likely be very difficult to achieve both good core recovery and sufficient quantity of the desired mineral phases to permit successful analysis of cores from that site (section 2). Since quartz-bearing bedrock appears to be absent in the Hudson Mountains (section 3.2), cosmogenic nuclide measurements will need to be undertaken on olivine and potentially plagioclase feldspar or clinopyroxene instead of quartz.

Our field survey revealed that quartz-bearing erratics − predominantly granites and granodiorite gneisses − are present on all nunataks in the Hudson Mountains, although their abundance varies markedly between nunataks. Considering the three remaining potential drill sites, erratic cobbles and boulders of granitoid lithology are very common at Winkie Nunatak and Maish Nunatak and exist, but are rare, at Webber Nunatak. Measurement of in situ ^{14}C in bedrock-erratic pairs for which the Holocene deglaciation history is already known (from [10]Be measurements of the erratics) would be a valuable tool for calibrating the local in situ ^{14}C production rate. The presence of abundant quartz-bearing erratics above the present ice margin at a site would thus benefit the analysis of subglacial bedrock cores from the same site, making nunataks where this is the case (Winkie and Maish nunataks) more desirable than those with scarce glacial deposits (Webber Nunatak). However, access to Maish Nunatak for any drilling campaign would be extremely challenging and likely insurmountable without helicopter support due to the presence of the active ablation zone adjacent to the nunatak. Therefore, and in summary, of the three leading drill sites surveyed, both Winkie and Webber nunataks are feasible, but Winkie Nunatak is much more desirable due to its lithology, easier accessibility (surface conditions are challenging at Webber Nunatak) and more conducive subglacial morphology.

4 Conclusions and recommendations

Bedrock cores collected from beneath the Antarctic Ice Sheet can provide evidence for ice sheet regrowth from a smaller-than-present configuration during the Holocene (Johnson et al., 2022; Balco et al., 2023). This paper outlines the criteria used for choosing a suitable site for subglacial bedrock drilling in the eastern Pine Island-Thwaites Glacier system. Two nunataks in

the Hudson Mountains were selected as feasible for subglacial drilling based on (i) their location proximal to the modern grounding line, (ii) the presence of outcropping ridges oriented perpendicular to modern ice flow and the likelihood that those ridges would have become more exposed if the grounding line had retreated inboard of present, iii) suitability of the bedrock lithology for cosmogenic nuclide analysis, and (iv) accessibility. These are Winkie Nunatak (74.86°S / 99.78°W) and Webber Nunatak (74.77°S / 99.83°W). Neither site is a perfect fit to all the criteria. However, Winkie Nunatak, with its olivine-rich bedrock lithology, well-consolidated structure and likely absence of overlying till on the subglacial ridge surface, is the highest scoring choice. In contrast, the presence of potentially permeable and less well-consolidated crystal-poor hyaloclastite bedrock at Webber Nunatak would make it challenging to retrieve subglacial samples, and those collected would likely not provide sufficient quantity of the target mineral (olivine) for cosmogenic nuclide measurement. Thus, we propose that Winkie Nunatak is the most suitable site for a subglacial drilling campaign aiming to detect Holocene retreat-readvance in the eastern Pine Island-Thwaites Glacier system.

This study provided an opportunity to reflect on our approach and consider how similar site surveys could be improved in future. We make the following recommendations for future assessments of suitability for subglacial bedrock drilling:

- Consult across a wide range of expertise (including drilling engineers, geophysicists, glaciologists and geologists as a minimum) when choosing a drill site, and discuss the available evidence as a group, not in isolation. This will ensure that issues that might affect different aspects of the work (e.g. drilling operations or sample analysis) are identified early and mitigations can be planned if needed.

- Ensure that sufficient field reconnaissance is undertaken (including obtaining rock samples and radar survey data) especially, as is often the case in remote parts of Antarctica, little is known about a site's geological and glaciological setting.

- Collect samples from the bedrock outcropping immediately above the candidate drill site, not just anywhere in the region, because lithologies and/or abundance and sizes of target minerals can vary dramatically between nunataks or even on individual ridges.

- GPR surveys should include detailed grids, not just single lines, because single line surveys may not adequately capture the ice thickness/bed conditions across the subglacial ridge extension. Consider also that ice conditions may have changed between the reconnaissance and drilling seasons, which may affect access as well as suitability for drilling.

- Prior to field reconnaissance, acquire model simulations (at as high resolution as possible) to determine how grounding-line retreat inboard of present would have affected ice sheet thickness and extent, had it occurred. Such simulations are valuable for predicting which sites are most likely to have become more exposed, and where, which informs the choice of drill site.

- Finally, in our experience it is unlikely that any one site will meet all the criteria and be completely ideal for drilling. Thus, discussion of the relative importance to the project's success of meeting each criterion is essential. Having a back-up site (or two) is also prudent, especially if conditions are likely to have changed since reconnaissance.

Postscript: Drilling at Winkie Nunatak was subsequently attempted in the 2022-23 season, but bedrock was not recovered. This outcome was due to factors unrelated to the choice of drill site, primarily a combination of weather conditions and logistical constraints that restricted the available time for drilling operations, and technical problems with clay transport and fluid circulation that made it impossible to penetrate a layer of mixed ice and till overlying the bedrock in the available time (see Braddock et al., 2024 for details). The metre-scale clay-rich ice/sediment layer could not have been detected in advance of drilling operations.

Appendix A

Method for radar survey and radar data analysis: A PulseEKKO 1000 GPR system with 200 MHz antennae was used to survey the snow surface at candidate drill sites. At Winkie Nunatak, a broad grid consisting of seven 400 m-long cross profiles was collected perpendicular to the ridge line, with the radar system towed on a wooden Nansen sledge behind a skidoo. These profiles were spaced at 100 m intervals away from the visible ridge line. A detailed grid of five 300 m-long lines was then collected at 25 m intervals along, and then parallel to, GPR line X-Y (Fig. 6). At Webber Nunatak, eight radar lines were collected perpendicular to the ridge expression at 50 m spacing, and one line was run away from the ridge tip through the centre of the grid. The lines increased in length from 150 m to 500 m with increasing distance from bedrock, due to the orientation of the steep ice slope running northwest, creating the rhomboid shape shown in yellow in Fig. 10. The skidoo travelled at 3-7 km/hr, with the system set to continuous collection mode with an in-field stack of 4. A hand-held Garmin GPS was used to locate the position of GPR survey lines.

Processing steps in the commercial GPR processing software package ReflexW (Sandmeier Scientific Software, version 7.2.2) included depth correction with a standard ice velocity of 0.168 m ns^{-1}, time-zero correction, background removal, high-pass frequency filtering (dewow), bandpass filtering and application of an energy-decay gain to compensate for geometric spreading losses in the radargram (cf. Daniels et al., 2004; Woodward et al., 2022). A number of migration algorithms were applied, which successfully removed artefacts at the bedrock reflector, but were unable to resolve crevasse edges clearly due to the irregular lineation of the crevasse tracks. Despite this, the distinctive GPR limbs from the largest crevasses allow crevasse location detection. The free, open-source seismic interpretation software OpendTect (2015) was employed to plot radargrams in real space using GPS coordinates. This enabled 3D analysis of GPR data and picking of the bedrock reflector. Picks were then exported into ESRI ArcScene to generate 3D plots of the ridge surface beneath the ice.

Author contributions

630 JSJ and JW undertook fieldwork in the Hudson Mountains and collected all the field observations and GPR data presented here. JSJ wrote the paper with assistance from GB (drilling operations) and JW (glaciology and radar). IN and KW processed the GPR data under the supervision of JW and SC. With the exception of Fig. 1 (see acknowledgements), JSJ and KW prepared all figures, with assistance from KAN and RAV. GB and BMG provided details of subglacial drilling equipment and methods, and the photographs shown in Fig. 3. JSJ, JW, SC, BMG, BH, DHR and GB obtained funding. All authors read and commented

635 on the manuscript.

Competing interests

The authors declare that they have no conflict of interest.

Data availability

All ground-penetrating radar data presented in the paper are publicly accessible in the UK Polar Data Centre at the following

640 link: https://doi.org/10.5285/9555694e-c9f5-4bf8-a556-2ad9d29e55c6 (Woodward and Johnson, 2024).

Acknowledgements

Logistical support for this work was provided by British Antarctic Survey (BAS) and United States Antarctic Program. We thank BAS Field Guides Tom King and Ashley Fusiarski for assistance in the field, and BAS Field Operations Managers Al Davies and Nick Gillett for managing the project logistics in Antarctica. Elena Field and Nathan Fenney (BAS) prepared field

645 maps. Laura Gerrish (BAS) helped prepare Figs. 1 and 4. John Fletcher (British Geological Survey, UK) prepared the rock thin sections shown in Figs. 7, 11 and 15, after samples were cut by Mark Evans (BAS). Eric Larour (NASA-Jet Propulsion Laboratory, USA) kindly provided data from model simulations used in Fig. 4. John Smellie (Leicester University, UK) provided valuable information about glaciovolcanic processes and their products. This work was undertaken for the "Geological History Constraints" project, a component of the International Thwaites Glacier Collaboration (ITGC) and

650 supported from the National Science Foundation (NSF: Grant OPP-1738989 and 2317097) and Natural Environment Research Council (NERC: Grants NE/S006710/1, NE/S006753/1 and NE/S00663X/1). GB was partially supported by the Ann and Gordon Getty Foundation. The LLNL contribution to this work was carried out under Contract DE-AC52-07NA27344. The paper is LLNL-JRNL-868777 and ITGC Contribution No. ITGC-126.

References

655   Arndt, J. E., Larter, R. D., Friedl, P., Gohl, K., Höppner, K., and the Science Team of Expedition PS104: Bathymetric controls on calving processes at Pine Island Glacier, The Cryosphere, 12, 2039–2050, https://doi.org/10.5194/tc-12-2039-2018, 2018.

Balco, G., Brown, N., Nichols, K. A., Venturelli, R. A., Adams, J. R., Braddock, S., Campbell, S. C., Goehring, B. M., Johnson, J. S., Rood, D. H., Wilcken, K., Hall, B. H., and Woodward, J.: Reversible ice sheet thinning in the Amundsen Sea Embayment
660   during the Late Holocene, The Cryosphere, https://doi.org/10.5194/tc-2022-172, 2023.

Balter-Kennedy, A., Schaefer, J. M., Briner, J. P., Young, N. E., Walcott, C., Kuhl, T., Moravec, E., Keisling, B. A., Anandakrishnan, S., Stevens, N., and Brown, N.: First Results from GreenDrill: Exposure dating in sub-ice material from Prudhoe Dome, northwestern Greenland. Abstract, AGU Fall Meeting, San Francisco, USA, 2023a.

665

Balter-Kennedy, A., Schaefer, J. M., Schwartz, R., Lamp, J. L., Penrose, L., Middleton, J., Hanley, J., Tibari, B., Blard, P.-H., Winckler, G., Hidy, A. J., and Balco, G.: Cosmogenic ^{10}Be in pyroxene: laboratory progress, production rate systematics, and application of the ^{10}Be–^{3}He nuclide pair in the Antarctic Dry Valleys, Geochronology, 5, 301–321, https://doi.org/10.5194/gchron-5-301-2023, 2023b.

670

Bergelin, M., Balco, G., Corbett, L. B., and Bierman, P. R.: Production rate calibration for cosmogenic ^{10}Be in pyroxene by applying a rapid fusion method to ^{10}Be-saturated samples from the Transantarctic Mountains, Antarctica, EGUsphere [preprint], https://doi.org/10.5194/egusphere-2024-702, 2024.

675   Bindschadler, R., Vornberger, P., Fleming, A. H., Fox, A. J., Mullins, J., Binnie, D., Paulsen, S. J., Granneman, B., and Gorodetzky, D.: The Landsat Image Mosaic of Antarctica, Remote Sensing of Environment, 112, 4214–4226, 2008.

Boeckmann, G. V., Gibson, C. J., Kuhl, T. W., Moravec, E., Johnson, J. A., Meulemans, Z., and Slawny, K.: Adaptation of the Winkie Drill for subglacial bedrock sampling, Ann. Glaciol., 62, 109–117, https://doi.org/10.1017/aog.2020.73, 2021.

680

Braddock, S., Hall, B. L., Johnson, J. S., Balco, G., Spoth, M., Whitehouse, P. L., Campbell, S., Goehring, B. M., Rood, D. H., and Woodward, J.: Relative sea-level data preclude major late Holocene ice-mass change in Pine Island Bay, Nat. Geosci., 15, 568–572, 2022.

685   Braddock, S., Venturelli, R. A., Nichols, K. A., Moravec, E., Boeckmann, G. V., Campbell, S., Balco, G., Ackert, R., Small, D., Johnson, J. S., Dunbar, N., Woodward, J., Mukhopadhyay, S., and Goehring, B.: Lessons learned from shallow subglacial bedrock drilling campaigns in Antarctica. Annals of Glaciology, https://doi:10.1017/aog.2024.12, 2024.

Carracedo, A., Rodés, Á., Smellie, J.L., Stuart, F.M.: Episodic erosion in West Antarctica inferred from cosmogenic ^{3}He and
690   ^{10}Be in olivine from Mount Hampton, Geomorphology, 327, 438–445, https://doi.org/10.1016/j.geomorph.2018.11.019, 2019.

Briner, J. P., Walcott, C., Schaefer, J. M., Young, N. E., MacGregor, J. A., Poinar, K., Keisling, B. A., Anandakrishnan, S., Albert, M. R., Kuhl, T., and Boeckmann, G.: Drill-site selection for cosmogenic-nuclide exposure dating of the bed of the Greenland Ice Sheet, The Cryosphere, 16, 3933–3948, https://doi.org/10.5194/tc-16-3933-2022, 2022.
695

Daniels, D. J.: Ground Penetrating Radar, 2nd edition. The Institution of Engineering and Technology, London, UK, 752 pp., ISBN 9780863413605, 2004.

Howat, I., Porter, C., Noh, M. -J., Husby, E., Khuvis, S., Danish, E., Tomko, K., Gardiner, J., Negrete, A., Yadav, B., Klassen,
700   J., Kelleher, C., Cloutier, M., Bakker, J., Enos, J., Arnold, G., Bauer, G., and Morin, P.: The Reference Elevation Model of Antarctica – Mosaics, Version 2, Harvard Dataverse, v1, 2022. doi: https://doi.org/10.7910/DVN/EBW8UC. [Accessed 15 May 2024]

Jeong, S., Howat, I. M., and Bassis, J. N.: Accelerated ice shelf rifting and retreat at Pine Island Glacier, West Antarctica,
705   Geophys. Res. Lett., 43 (22), 11720–11725, https://doi.org/10.1002/2016GL071360, 2016.

Johnson, J. S., Bentley, M. J., and Gohl, K.: First exposure ages from the Amundsen Sea Embayment, West Antarctica: The Late Quaternary context for recent thinning of Pine Island, Smith, and Pope Glaciers, Geology, 36(3), 223–226, 2008.

710   Johnson, J. S., Bentley, M. J., Smith, J. A., Finkel, R. C., Rood, D. H., Gohl, K., Balco, G., Larter, R. D., and Schaefer, J. M.: Rapid thinning of Pine Island Glacier in the early Holocene. Science, 343, 999–1001, 2014.

Johnson, J. S., Nichols, K. A., Goehring, B. M., Balco, G., and Schaefer, J. M.: Abrupt mid-Holocene ice loss in the western Weddell Sea Embayment of Antarctica, Earth Planet. Sc. Lett., 518, 127–135, https://doi.org/10.1016/j.epsl.2019.05.002,
715   2019.

Johnson, J. S., Pollard, D., Whitehouse, P. L., Roberts, S. J., Rood, D. H., and Schaefer, J. M.: Comparing glacial-geological evidence and model simulations of ice sheet change since the Last Glacial Period in the Amundsen Sea sector of Antarctica, J. Geophys. Res.-Earth., 126, e2020JF005827, https://doi.org/10.1029/2020JF005827, 2021.

720

Johnson, J. S. and Smellie, J. L.: Zeolites compositions as proxies for eruptive palaeoenvironment, Geochem. Geophy. Geosy., 8, Q03009, 10.1029/2006GC001450, 2007.

Johnson, J. S., Venturelli, R. A., Balco, G., Allen, C. S., Braddock, S. C., Campbell, S., Goehring, B. M., Hall, B. L., Neff, P.

725   D., Nichols, K. A., Rood, D. H., Thomas, E.R., and Woodward, J.: Existing and potential evidence for Holocene grounding-line retreat and readvance in Antarctica, The Cryosphere, https://doi.org/10.5194/tc-16-1543-2022, 2022.

Jones, R. S., Johnson, J. S., Lin, Y., Mackintosh, A. N., Sefton, J. P., Smith, J. A., Thomas, E. R., and Whitehouse, P. L.: Stability of the Antarctic Ice Sheet during the pre-industrial Holocene, Nat. Rev. Earth Environ.,

730   https://doi.org/10.1038/s43017-022-00309-5, 2022.

Joughin, I., Smith, B. E., and Medley, B.: Marine ice sheet collapse potentially under way for the Thwaites Glacier Basin, West Antarctica, Science, 344, 735–738, https://doi.org/10.1126/science.1249055, 2014.

735   Joughin, I., Shapero, D., Smith, B., Dutrieux, P., and Barham, M.: Ice-shelf retreat drives recent Pine Island Glacier speedup, Science Advances, 7, eabg3080, https://www.science.org/doi/10.1126/sciadv.abg3080, 2021.

Kingslake, J., Scherer, R., Albrecht, T., Coenen, J., Powell, R.D., Reese, R., Stansell, N.D., Tulaczyk, S., Wearing, M.G., and Whitehouse, P.L.: Extensive retreat and re-advance of the West Antarctic Ice Sheet during the Holocene, Nature, 558, 430–

740   434, 2018.

Koester, A. J. and Lifton, N. A.: Technical note: A software framework for calculating compositionally dependent in situ ^{14}C production rates, Geochronology, 5, 21–33, https://doi.org/10.5194/gchron-5-21-2023, 2023.

745   Kuhl, T., Gibson, C., Johnson, J., Boeckmann, G., Moravec, E., and Slawny, K.: Agile Sub-Ice Geological (ASIG) Drill development and Pirrit Hills field project, Annals of Glaciology, 1–14, https://doi.org/10.1017/aog.2020.59, 2020.

Lamp, J. L., Young, N. E., Koffman, T., Schimmelpfennig, I., Tuna, T., Bard, E., and Schaefer, J. M.: Update on the cosmogenic in situ ^{14}C laboratory at the Lamont-Doherty Earth Observatory, Nuclear Instruments and Methods in Physics

750 Research Section B: Beam Interactions with Materials and Atoms, 456, 157–162, https://doi.org/10.1016/j.nimb.2019.05.064, 2019.

Larour., E., Seroussi, H., Morlighem, M., and Rignot, E.: Continental scale,high order, high spatial resolution, ice sheet modeling using the Ice Sheet System Model (ISSM), J. Geophys. Res., 117, F01022, 2012.

755

Larour, E., Seroussi, H., Adhikari, S., Ivins, E., Caron, L., Morlighem, M., and Schlegel, N.: Slowdown in Antarctic mass loss from solid Earth and sea-level feedbacks, Science, 364, eaav7908, 2019.

Lifton, N., Jull, A., and Quade, J.: A new extraction technique and production rate estimate for in situ cosmogenic ^{14}C in 760 quartz, Geochimica et Cosmochimica Acta, 65(12), 1953–1969, 2001.

Lopatin, B. G. and Polyakov, M. M.: Geology of the volcanic Hudson Mountains (Walgreen Coast, West Antarctica) (in Russian), Antarkt. Dokl. Komissii, 13, 36-51, 1974.

765 Mackintosh, A. White, D., Fink, D., Gore, D. B., Pickard, J., and Fanning, P. C.: Exposure ages from mountain dipsticks in Mac. Robertson Land, East Antarctica, indicate little change in ice-sheet thickness since the Last Glacial Maximum. Geology, 35 (6), 551–554. https://doi.org/10.1130/G23503A.1, 2007.

Mas e Braga, M., Jones, R. S., Newall, J. C. H., Rogozhina, I., Andersen, J. L., Lifton, N. A., and Stroeven, A. P.: Nunataks 770 as barriers to ice flow: implications for palaeo ice sheet reconstructions, Cryosphere, 15, 4929–4947, https://doi.org/10.5194/tc-15-4929-2021, 2021.

Meredith, M., Sommerkorn, M., Cassotta, S., Derksen, C., Ekaykin, A., Hollowed, A., Kofinas, G., Mackintosh, A., Melbourne-Thomas, J., Muelbert, M. M. C., Ottersen, G., Pritchard, H., and Schuur, E. A. G.: Chapter 3: Polar Regions. In: 775 IPCC Special Report on the Ocean and Cryosphere in a Changing Climate [Pörtner, H. -O., Roberts, D. C., Masson-Delmotte, V., Zhai, P., Tignor, M., Poloczanska, E., Mintenbeck, K., Alegría, A., Nicolai, M., Okem, A., Petzold, J., Rama, B., Weyer, N. M. (eds.)]. Cambridge University Press, Cambridge, UK and New York, NY, USA, 203–320, https://doi.org/10.1017/9781009157964.005, 2019.

780 Mukhopadhyay, S.: "Ohio Range Subglacial rock core cosmogenic nuclide data" U.S. Antarctic Program (USAP) Data Center, doi: https://doi.org/10.15784/601351, 2020.

Nias, I. J., Cornford, S. L., Edwards, T. L., Gourmelen, N., and Payne, A. J.: Assessing uncertainty in the dynamical ice response to ocean warming in the Amundsen Sea Embayment, West Antarctica, Geophys. Res. Lett., 46, 785 https://doi.org/10.1029/2019GL084941, 2019.

Nichols, K. A.: A decade of in situ cosmogenic ^{14}C in Antarctica, Annals of Glaciology, 63 (87–89), 67–72, https://doi.org/10.1017/aog.2023.13, 2022.

790 Nichols, K. A., Rood, D. H., Venturelli, R. A., Balco, G., Adams, J., Guillaume, L., Campbell, S., Goehring, B. M., Hall, B. M., Wilcken, K., Woodward, J. W., and Johnson, J. S.: Offshore-onshore record of Last Glacial Maximum-to-present grounding line retreat at Pine Island Glacier, Geology 51(11), 1033–1037, https://doi.org/10.1130/G51326.1, 2023.

Pigati, J. S., Lifton, N. A., Jull, A. J. T., and Quade, J.: Extraction of In Situ Cosmogenic ^{14}C from olivine, Radiocarbon, 52, 795 1244–1260, https://doi.org/10.1017/S0033822200046336, 2010.

Rignot, E., Mouginot, J., and Scheuchl, B.: MEaSUREs Antarctic Grounding Line from Differential Satellite Radar Interferometry, Version 2. Boulder, Colorado USA. NASA National Snow and Ice Data Center Distributed Active Archive Center, 2016. doi: https://doi.org/10.5067/IKBWW4RYHF1Q [16 May 2024]

800

Rignot, E., Mouginot, J., and Scheuchl, B.: MEaSUREs InSAR-Based Antarctica Ice Velocity Map, Version 2. Boulder, Colorado USA, NASA National Snow and Ice Data Center Distributed Active Archive Center, 2017. doi: https://doi.org/10.5067/D7GK8F5J8M8R [16 May 2024]

805 Rowley, P. D., Laudon, T. S., LaPrade, K. E., and LeMasurier, W. E.: Hudson Mountains, In: Volcanoes of the Antarctic Plate & Southern Oceans, LeMasurier, W. E. & Thomson, J. W. (eds.). Antarctic Research Series 48, 289–293, 1990.

Schaefer, J. M., Finkel, R. C., Balco, G., Alley, R. B., Caffee, M. W., Briner, J. P., Young, N. E., Gow, A. J., and Schwartz, R.: Greenland was nearly ice-free for extended periods during the Pleistocene, Nature 540, 252–255, 2016.

810

Small, D., Smedley, R., Dunai, T., Lees, T., Trabucatti, S., and Boeckmann, G.: New geological constraints on Holocene retreat-readvance of the West Antarctic Ice Sheet in the Weddell Sea Embayment, EGU General Assembly 2024, Vienna, Austria, 14–19 Apr 2024, EGU24-12136, https://doi.org/10.5194/egusphere-egu24-12136, 2024.

815   Smith, B., Fricker, H. A., Gardner, A. S., Medley, B., Nilsson, J., Paolo, F. S., Holschuh, N., Adusumilli, S., Brunt, K., Csatho, B., Harbeck, K., Markus, T., Neumann, T., Siegfried, M. R., and Zwally, H. J.: Pervasive ice sheet mass loss reflects competing ocean and atmosphere processes, Science, 368(6496), 1239–1242, https://doi.org/10.1126/science.aaz5845, 2020.

Spector, P., Stone, J., Pollard, D., Hillebrand, T., Lewis, C., and Gombiner, J.: West Antarctic sites for subglacial drilling to
820   test for past ice-sheet collapse, The Cryosphere, 12, 2741–2757, https://doi.org/10.5194/tc-12-2741-2018, 2018.

Spector, P., Stone, J., and Goehring, B.: Thickness of the divide and flank of the West Antarctic Ice Sheet through the last deglaciation, The Cryosphere, 13, 3061–3075, https://doi.org/10.5194/tc-13-3061-2019, 2019.

825   Stone, J. O., Balco, G. A., Sugden, D. E., Caffee, M. W., Sass, L. C., Cowdery, S. G., and Siddoway, C.: Holocene deglaciation of Marie Byrd Land, West Antarctica, Science, 299, 99–102, 2003.

Stroncik, N. A. and Schmincke, H. U.: Palagonite – a review, Int. J. Earth Sci., 91, 680–697, https://doi.org/10.1007/s00531-001-0238-7, 2002.
830
Venturelli, R. A., Siegfried, M. R., Roush, K. A., Li, W., Burnett, J., Zook, R., Fricker, H. A., Priscu, J. C., Leventer, A., and Rosenheim, B. E.: Mid-Holocene Grounding Line Retreat and Readvance at Whillans Ice Stream, West Antarctica, Geophys. Res. Lett., 47 (15), https://doi.org/10.1029/2020GL088476, 2020.

835   Venturelli R. A., Boehman, B., Davis, C., Hawkings, J. R., Johnston, S. E., Gustafson, C. D., Michaud, A. B., Mosbeux, C., Siegfried, M. R., Vick-Majors, T. J., Galy, V., Spencer, R. G. M., Warny, S., Christner, B. C., Fricker, H. A., Harwood, D. M., Leventer, A., Priscu, J. C., Rosenheim, B. E., and SALSA Science Team: Constraints on the timing and extent of deglacial grounding line retreat in West Antarctica, AGU Advances 4, e2022AV000846, https://doi.org/10.1029/2022AV000846, 2023.

840   White, J. D. L. and Houghton, B. F.: Primary volcaniclastic rocks. Geology, 34, 677–680, 2006.

Woodward, J. W., Hein, A. S., Winter, K., Westoby, M. J., Marrero, S. M., Dunning, S. A., Lim, M., Rivera, A., and Sugden, D. E.: Blue-ice moraines formation in the Heritage Range, West Antarctica: Implications for ice sheet history and climate reconstruction, Quaternary Sci. Adv., 6, 100051, https://doi.org/10.1016/j.qsa.2022.100051, 2022.
845
Woodward, J. and Johnson J. S.: Ground-penetrating radar surveys at three nunataks in the Hudson Mountains in the Amundsen Sea sector of West Antarctica, December 2019 (version 1.0) [Data set], NERC EDS UK Polar Data Centre, https://doi.org/10.5285/9555694e-c9f5-4bf8-a556-2ad9d29e55c6, 2024.